SSS-R-77-3145

FE-1770-23
Distribution Category UC-90c

COMPUTER MODELING OF COAL GASIFICATION REACTORS

Quarterly Technical Progress Report
For Period October 1, 1976 - December 31, 1976

Thomas R. Blake

February 1977

Under Contract No. E(49-18)-1770

PREPARED FOR
ENERGY RESEARCH AND DEVELOPMENT ADMINISTRATION

Systems, Science and Software
P. O. Box 1620
La Jolla, California 92038

TABLE OF CONTENTS

ABSTRACT

This report presents a summary of the work accomplished during the sixth quarter of a three year study conducted for the U.S. Energy Research and Development Administration under Contract No. E(49-18)-1770. The objective of this research is to develop and apply computer codes, based upon continuum theories of multiphase, reactive flows, to the performance of fluidized bed and entrained flow reactors for coal gasification.

I. OBJECTIVE AND SCOPE OF WORK

The purpose of this program is to develop and apply, over three years, accurate and general computer models that will expedite the development and aid in the optimization and scale-up of reactors for coal gasification. Initial applications will be to fluidized bed gasification processes; subsequently both entrained flow reactors and fast fluidized beds will be examined.

During the first year, work will be initiated on the fluidized bed model in the areas of multiphase fluid flow without chemical reactions, and chemical reactions without fluid flow. The computer codes, developed to represent these aspects of gasification processes, will be combined in the second year of the program into a numerical model of reactive flows in fluidized beds. This model will provide a time-dependent field description of fluidized bed flows in two space dimensions. Calculations will be performed with the prototype code during the first and second years to verify the accuracy of the formulations employed and, in the second year, these calculations should provide preliminary results relevant to coal gasifications. During the second year a computer model for entrained flow gasifiers will be formulated and the chemistry defined; this model will provide a field description of entrained flows in two space dimensions. Nonreactive flow calculations will be performed for entrained flow processes at the end of the second year.

In the third year the application of the fluidized bed computer model to specific gasifier processes will be extended and a computational model which includes three-dimensional effects will be developed. Also, during this third year the coal chemistry will be combined with the entrained flow computer model and some calculations of such gasifier configurations will be performed.

II. SUMMARY OF PROGRESS TO DATE

This was the second quarter in the second year of research to develop and apply computer codes, based upon continuum theories of multiphase flows, to the performance of fluidized bed and entrained flow coal gasification reactors. Research was active in several areas.

The research on the fluidized bed computer code included the development of the models for the heterogeneous and homogeneous reactions appropriate to char combustion and the incorporation of that chemistry into source and transport terms for the conservation equations. These source terms will be included in the numerical model in the next quarter. The basic numerical code was modified to reduce computer core requirements and to thereby permit the calculation of problems with a large number of zones. Parametric calculations were performed with this code to represent the influences of bed geometry, mass flow rate and distribution and hydrostatic pressure effects in fluidized beds.

The work on the entrained flow computer model involved both the formulation of the basic conservation equations and the development of a computer code to test possible numerical techniques appropriate for that system of conservation equations. These conservation equations represent turbulent compressible flow of gas and solid particles, including the influence of chemical reactions. Constitutive equations for these turbulent flows are being formulated. The computer code is a finite element-finite difference code which treats a system of equations mathematically like that for entrained flow and it is being used to investigate the application of finite element techniques to the computer modeling of such flows.

III. DETAILED DESCRIPTION OF TECHNICAL PROGRESS

3.1 TASK 00 - MANAGEMENT, DOCUMENTATION AND CONSULTING

A review of the fluidized bed computer model was presented at the ERDA-Fossil Energy Conference on Computerized Mathematical Modeling of Coal Conversion Processes on November 16, 1976.

The AIChE Annual Meeting in Chicago, November 30-December 7, 1976, was attended. We presented a paper, "A Numerical Model of Gas Fluidized Beds", wherein we summarized some of the theoretical and numerical aspects of the model and examined some parametric calculations. This paper has subsequently been accepted for publication in the AIChE Progress Symposium Series.

Professor C. Y. Wen of West Virginia University consulted with S^3 staff members on the subjects of fluidization and coal chemistry. He has agreed to develop a quasi-homogeneous reactor model which will serve as a numerical representation of steam oxygen gasification chemistry in a simple flow environment. This effort, through West Virginia University, will be supported by a subcontract which has been written and submitted to ERDA for approval.

Professor Paul A. Libby of the University of California, San Diego, is consulting on the subjects of reactive turbulent flows and the evolution of particle size distribution in such flows. This research is related to our development of the computer model for entrained flow gasification.

During this past quarter, close liaison between Systems, Science and Software and other industrial and research organizations in coal gasification was maintained through visits and discussions on the subjects of both fluidized bed and entrained flow gasification.

3.2 TASK 01 - FLUIDIZED BED COAL GASIFICATION MODEL

The research on the fluidized bed model was directed to the development of the chemistry for steam-oxygen gasification processes and to the development and application of the fluidized bed computer code.

The formulation of the chemistry for heterogeneous and homogeneous reactions for char gasification and combustion was continued. The representation of those reactions appropriate to char combustion was essentially completed and is summarized

in Appendix A. The nature of this formulation is analogous to the development of the thermomechanical constitutive equations and mechanical interaction terms in the continuum model [c.f., Blake, et al., 1976]. We use theoretical and and experimental representations of the heterogeneous and homogeneous reaction kinetics together with relationships for species transport to develop appropriate source and flux terms for the equations of mass and energy balance. In the case of the heterogeneous reactions, we consider the balance of gas-solid mass transport, represented by film diffusion, and the kinetic processes of adsorption and desorption, represented by a Langmuir isotherm, for a single particle. This determines an overall reaction rate (say: gms of carbon removed/cm^2 of particle surface area/sec) which, when summed over all local particles, provides a mass source term for the differential equations describing conservation of mass. In a similar manner, this exchange of mass between the gas and solid particles contributes to the energy balance for the two phases. The influence of such exchange upon the individual particles is included in Lagrangian differential equations for particle size and particle temperature. The homogeneous reactions appropriate to combustion, such as volatiles oxidation and water gas shift, are represented by volumetric source terms in the conservation of mass for the respective gas species. These volumetric integrals reflect both the local gas properties through the kinetics and the local volume fraction occupied by the gas phase. The influence of these homogeneous reactions upon the energy balance for the gas phase is accounted for by incorporating the heat of formation in our definition of specific internal energy for each constituent. These reactions for char combustion will be incorporated into the fluidized bed code in the following quarter and the formulation of the additional chemistry for gasification and devolatilization will be continued. In the latter case, we expect to utilize aspects of the chemistry on gasification and devolatilization which were developed in the first year of this effort [Blake, et al., 1976]. Further, the homogeneous reactor model to be developed by West Virginia University will provide a simple numerical environment in which we shall test the sensitivity of the chemistry to changes in chemical parameters for combustion, gasification and devolatilization/prompt methanation.

Within the context of homogeneous reactor models, we note that aspects of the chemistry model for the CO_2 acceptor process, developed at S^3 in the first year, will be used in the planned West Virginia effort. Both that previous model and the future effort contain chemistry and numerical methodology which will be used, in part, in the incorporation of chemistry into our multidimensional fluidized bed

computer model. A draft topical report has been prepared which documents the S^3 homogeneous reactor model of the CO_2 acceptor process. This report, which discusses the code modifications since the publication of our annual report [Blake, et al., 1976] will be submitted to ERDA for review.

Research was continued on the hydrodynamic and transport aspects of the multidimensional fluidized bed computer model; this research included code development, formulation of representations of particle size effects on transport and parametric numerical studies. A major effort was initiated and completed to reduce the computer core requirements for the numerical model. This activity, which is part of a continuing effort to make the code more efficient, will permit the calculation of problems with an increased number of zones in the finite difference grid. Further, such a reduction in core requirements means that the added complexity associated with the chemistry and multi-component species transport of reactive flows can be more readily treated.

Parametric variations in fluidized bed flows were studied with the two-dimensional fluidized bed computer model. The influence of bed height/width ratio, mass flow rate, mass flow distribution and bed hydrostatic pressure were examined with a limited number of calculations. These calculations, which are briefly summarized in Appendix B, were presented and discussed in our review presentation at ERDA on November 16, 1976.

A theoretical formulation describing the relative transport of particles of different sizes in the fluidized bed was initiated. In that representation, the properties of the fluidized bed such as solid phase viscosity, solid phase pressure, solid particle-gas drag relationship, etc. are assumed to be determined by an average of the particle size distribution. Then for each discrete particle size, the motion of that particle size, with respect to this average bed, is calculated by appropriate dynamic relationships. Such a calculation can be performed for each discrete size (likely the particle size distribution would be divided into a finite number of "bins" of particles by size range) to determine the relative motion of large and small particles in the bed. A related approach would be to calculate the evolution of a particle size distribution. Such an effort has been initiated for entrained flows (c.f., Section 3.3) and it may be possible to apply similar techniques to fluidized beds. However, in the case of fluidized bed flows, there is strong particle-particle and particle-gas interaction which requires the definition of collisional terms in such a representation of particle size distribution;

those terms, which involve mechanisms of significant coupling between the particle size distribution and the flow field are, in general, complicated.

3.3 TASK 02 - ENTRAINED FLOW COAL GASIFICATION MODEL

The research on the entrained flow model included a continued formulation of the conservation equations for turbulent gas-solid particle motion and the development of a numerical model to test methodology of finite element-finite difference solutions for a model system of equations.

In the previous quarter [Blake, 1976], we considered the balance equations for gas-solid particle flows without turbulence. For entrained flows, the solid particle loading is relatively small compared with, say, the emulsion phase of fluidized beds. This means that the conservation equations for entrained flows, in contrast with those for fluidized processes, must include the inertia of both the gas andsolid phases and may exclude particle-particle interaction terms. Further, the regime of entrained flow, important to coal gasification reactors, is a turbulent regime wherein the respective influences of gas and particle effects must be accounted for. We have incoporated turbulence into our balance equations for entrained flows and we discuss this formulation in Appendix C. We introduce a modified Favre average to account for compressibility in the flow and develop conservation equations for the gas and solid phases which include the influences of chemical reactions. Specific approximations and closure requirements for this system of equations have been examined. We expect to use a differential representation of the turbulence based upon an extrapolation of concepts from turbulence in fluids and gases without particles.

The evolution of particle size distributions in either inert or reactive entrained flows must be accounted for in our numerical model. One possible approach is to formulate a differential equation for the number of particles at location x_i, time t, radius r, velocity u_i, and temperature, T_p. The calculation of such a number density, or particle size distribution, would be accomplished as part of the coupled system of equations for entrained flows. Obviously, this is not a trivial problem. We have initiated a study of the evolution of particle size distribution for entrained flows. A summary of this initial study is presented in Appendix D; it is assumed that the total number of particles is sufficiently small so that the characteristics of the gas flow are unaffected and therefore are known. The influence of a turbulent, chemically active carrier gas upon the particle

size distribution is included in the formulation and methods of solution have been examined. The extension of this treatment to the case of the coupled problem, wherein the particles have a significant influence upon the carrier gas is being examined and some aspects of this case are presented in Appendix D.

There are many finite difference techniques which might be used to treat the case of transient, turbulent entrained flows. Some aspects of flow in gasifiers particularly as related to the geometry of connecting spools, injection nozzles, etc. indicate that finite element techniques might be a useful method of solution. In order to provide a reasonable basis to examine this issue, we have developed a finite element-finite difference code for transient flow of a compressible viscous gas. It is easy to show that the mathematical character of the system of equations for such flows is identical to that for the more complicated entrained flows under consideration. Hence, the finite element formulation permits us to examine the applicability and flexibility of such a method to the problem of interest. Further, numerical methodology related to both the boundary conditions and the differential equations for viscous compressible flow can be directly applied to the entrained flow model. Our present conclusions are that the finite element technique does offer advantages as compared to finite difference approaches, however, we will be examining this question further in the following quarter. A discussion of the finite element-finite difference technique and some simple calculations are presented in Appendix E.

IV. CONCLUSIONS

In summary, we note the following aspects of our modeling effort.

- Existing data and theoretical models related to heterogeneous char combustion and the associated homogeneous reactions can be naturally incorporated into our continuum model for fluidized beds.

- Theoretical formulations for particle size distribution and particle dynamics have been initiated which potentially can lead to a general description of particle size influences in both fluidized beds and entrained flows.

- A turbulence formulation is being developed for entrained flows which is both related to existing concepts of turbulence without particles and can also provide a description of the coupled behavior of particles and gas in turbulent entrained flows.

- An examination of numerical methods for the solution of the differential equations of entrained flow indicates that both finite element and finite difference techniques have distinct advantages. The former method seems particularly appropriate in the treatment of complex geometries.

APPENDIX A
OXIDATION REACTIONS

INTRODUCTION

The combustion of char and the associated oxidation reactions in the gaseous phase provide the source of heat for processes of steam oxygen gasification. In the following paragraphs we examine these heterogeneous and homogeneous reactions and discuss the incorporation of the chemistry into the conservation equations for gas fluidized beds. The nature of this formulation is analogous to that already developed for the constitutive and mechanical interaction terms in the fluidized bed equations [c.f., Blake, et al., 1976]; based upon theoretical and experimental representation of the heterogeneous and homogeneous reactions, appropriate source and flux terms are derived for the mass and energy conservation equations.

Heterogeneous reactions involve discrete physicochemical processes which contribute to the overall reaction rate [Rosner, 1972; Walker, et al., 1959; Wheeler, 1951; Weisz and Prater, 1954]. These physicochemical influences are more complicated in the case of char because of changes in the time history of the char particle structure during the course of the reaction [Mulcahy and Smith, 1969]. While the oxidation reactions of carbon, coal and char are perhaps the most extensively documented reactions in coal chemistry, there is still significant controversy with respect to the dominant reaction mechanisms [c.f., Gray, et al., 1974; Mulcahy and Smith, 1969; Essenhigh, et al., 1965]. For example the definitions of reaction order and the associated activation energy in the interpretation of experimental data is still to be completely resolved. Essenhigh and his coworkers have noted that there is a logical difficulty in the

assumption of a high activation energy with a near unity reaction order. Such questions are directly related to the respective influences of pore diffusion and the adsorption-desorption processes. In the present development we will use a Langmuir isotherm to represent the chemical reaction rate, in terms of adsorption and desorption processes, and assume that the rate of reactant diffusion from the ambient gas to the particle surface is balanced by the rate of chemical reaction. We will not explicitly account for pore diffusion. However, we note that the influence of pore diffusion can be described by modified velocity constants for adsorption and desorption [Walker, et al., 1959; Thring and Essenhigh, 1963]. Further, we note that, in addition to the excellent representation of data on carbons [Essenhigh, et al., 1965; Tu, et al., 1934] and chars [Gray, et al., 1974; Field, 1969] not exhibiting pore diffusion control, the Langmuir isotherm also provides a good representation of the temperature dependence of data for chars and coals of different ranks [Dobner, 1976; Smith, 1971a, 1971b; Field, 1970]. Within this context we essentially view the application of the Langmuir formulation as a semiempirical representation of the data. The coefficients in the Langmuir isotherm are defined from these combustion data on small particles of coal, carbon and char, where the resistance is dominated by the adsorption and desorption processes. For larger particles [c.f., Nettleton, 1967; Field, et al., 1967; Field, 1969; Mulcahy and Smith, 1969; Essenhigh, et al., 1965; Avedesian and Davidson, 1973] mass transport to the particle can control, and is described by a diffusional resistance which is dependent upon the Reynolds and Prandtl numbers.

In the present study we use data and models for single particle char combustion to describe mass and energy exchange between the individual particles and the gas phase. Then, the

influence of many particles upon the continuum model [Blake, et al., 1976] of fluidized bed flow is obtained by summing over all the particles. This summation leads to the definition of source terms in the conservation equations describing the continuum model. For simplicity in the present discussion we consider that the char particles are carbon and that they are spherical. The addition of other species is a simple matter and the nonspherical nature of the particles can be included in a manner similar to our use of shape factors in the mechanical interaction terms of the model.

CHAR COMBUSTION

There are primarily four controlling steps in heterogeneous reactions [c.f., Walker, et al., 1959; Mulcahy and Smith, 1969; Rosner, 1972] which reflect the respective influences of mass transport, chemisorption and desorption. These steps are:

1. Mass transport of reactants and product gases between the exterior surface of particle and external gas flow.
2. Mass transport of reactants and products between the exterior surface of particle and active site within the particle.
3. Chemisorption of reactant at the active site.
4. Desorption of products at the active site.

The relative dominance of these steps is of prime importance in the apparent order and activation energy of the reaction. For carbon and coal char combustion it is expected that the process of desorption controls at low temperatures; the reaction is zero order in the partial pressure of oxygen and there is an activation energy of approximately 40 kcal/mol [Gray, et al., 1974; Hamor, et al., 1973; Smith, 1971a; Smith 1971b; Mulcahy and Smith, 1969; Field, et al., 1967; Essenhigh, et al.,

1965]. At the higher temperatures the reaction tends to be first order and has a low activation energy of approximately 10 kcal/mol. This has been interpreted [Dobner, 1976; Gray, et al., 1974; Essenhigh, et al., 1965] as a regime in which adsorption controls. Between these high and low temperature regimes, influences of pore diffusion upon reaction order and activation energy have been observed. The temperature region for pore diffusion control appears to be a function of coal rank [c.f., Gray, et al., 1974; Hamor, et al., 1973; Field, 1970, 1969; Smith 1971a,b] and is likely related to the respective pore structure in the particles.

For small particles (<100 μ) the influence of mass transport to the particle is less than that of the other three steps in the reaction process; however, it must be included in the interpretation of the data because in many cases it is not negligible [c.f., Smith 1971a,b]. For larger particles (>100 μ) the mass transport of reactants to the particle can control so the combustion process becomes diffusion controlled.

It is possible for carbon to react with oxygen to form both carbon monoxide and carbon dioxide. Investigations on carbons with rather different reactivities [Walker, et al., 1959; Arthur, 1951] suggest that the ratio of CO to CO_2 formed in combustion is a strong function of temperature and that for the higher temperature range, appropriate to coal gasification, carbon monoxide is the primary product. We will, therefore, consider that the heterogeneous combustion reaction is

$$C + \frac{1}{2} O_2 \rightarrow CO \qquad (R1)$$

Further we will assume that the oxidation of the carbon monoxide

$$CO + \frac{1}{2} O_2 \rightleftarrows CO_2 \qquad (R2)$$

occurs outside of the particle [Field, 1969; Batchelder, 1953]. This means that we neglect any heating of the particle which could occur by oxidation of CO within the pore structure of the particle. Such oxidation has been observed in an oxygen rich environment by Froberg [c.f., Gray, et al., 1974] and Kurylko and Essenhigh, 1972. Further, the presence of CO_2 in the gas can lead to gasification of the carbon and to a subsequent production of carbon monoxide. This effect has been discussed by Field, et al., 1967 for pulverized coal. While the definition of the reaction rate for the carbon-carbon dioxide reaction is still the subject of investigation, present estimates indicate that it is slow compared to the oxidation reactions. If one uses the reaction rates discussed by Dobner, 1976 [c.f., Gray and Kimber, 1967], this reaction is two to three orders of magnitude slower than the oxidation of carbon and, most important, it is, for particles less than 1 cm, much slower than the rate of diffusion of reactants to the particle. We shall, therefore, neglect the carbon-carbon dioxide reaction in the combustion of char. We note that for some cases of diffusion controlled carbon combustion, both Avedesian and Davidson, 1973 and Kurylko and Essenhigh, 1972 invoke such a gasification reaction. The relative importance of the carbon-carbon dioxide reaction to combustion of larger particles ($\geq$ 1 cm) is, in our view, uncertain; however, for both species and energy balance, in diffusion controlled combustion, the combination of R1 for the heterogeneous reaction and R2 for the homogeneous reaction is equivalent to the combination of the carbon-carbon dioxide gasification reaction with R2 for the homogeneous reaction.

The presence of steam in the gas phase must be accounted for and hence the reaction

$$H_2 + \frac{1}{2} O_2 \rightleftharpoons H_2O \qquad \text{(R3)}$$

is important. This reaction is maintained close to equilibrium [c.f., Batchelder, 1953] and so the presence of H_2O tends to augment the concentration of O_2. Further, equilibrium in R2 and R3 imposes water gas shift equilibrium on the gas phase. However, in general we must include the water gas shift reaction so we write

$$H_2O + CO \rightleftarrows CO_2 + H_2 \qquad \text{(R4)}$$

Finally, we note that the reaction of steam with solid carbon is neglected because its rate is of the order of the carbon-carbon dioxide gasification reaction. It is therefore much slower than the combustion reaction R1, and is also slower than the reactant transport to the particle for $r \leq 1$ cm [Batchelder, 1953; Field, et al., 1967; Gray and Kimber, 1967].

HETEROGENEOUS REACTION, LANGMUIR ISOTHERM

For a char particle the rate of combustion of char (gms/cm^2-sec) is represented by the Langmuir isotherm

$$\dot{R}_c = \frac{K_1 \, P\acute{o}_2}{1 + \frac{K_1}{K_2} P\acute{o}_2} \qquad \text{(A1)}$$

where K_1 and K_2 are the velocity coefficients, describing, respectively, adsorption and desorption and $P\acute{o}_2$ is the partial pressure of oxygen at the particle surface. These velocity coefficients are functions of temperature

$$K_1 = A_1 \exp - \frac{E_1}{RT}$$
$$K_2 = A_2 \exp - \frac{E_2}{RT} \qquad \text{(A2)}$$

where E_1 and E_2 are activation energies and the coefficient A_1 and A_2 can be functions of temperature. For reaction R1, the consumption of one mole of carbon requires one-half mole

of oxygen. The molar flux of oxygen to the surface (moles/cm^2 sec) is

$$J_{O_2} = - \frac{D_o}{RT} \left(\frac{T}{T_o}\right)^n \frac{Sh}{2r} (P\acute{o}_2 - Po_2) \qquad (A3)$$

where D_o is the binary diffusion coefficient for oxygen at reference temperature T_o, Sh is the Sherwood number, r is the particle radius, T´ is the particle temperature, T is the free stream temperature and Po_2 is the free stream partial oxygen pressure. The Sherwood number can be related to Reynolds and Schmidt numbers by the semiempirical expression

$$Sh = 2 + A\, Re^B Sc^C \qquad (A4)$$

where Re is defined in terms of the relative particle-gas velocity. These equations are standard relationships; Essenhigh, et al., 1965; Field, et al., 1967 and Mulcahy and Smith, 1969 review the literature and define the constants n, A, B and C within the context of char combustion.

For the reaction R1, the Equations (A1) and (A3) can be combined to give

$$- \frac{2M_c D_o}{RT} \left(\frac{T}{T_o}\right)^n \frac{Sh}{2r} (P\acute{o}_2 - Po_2) =$$

$$\frac{K_1\, P\acute{o}_2}{1 + \frac{K_1}{K_2} P\acute{o}_2} \qquad (A5a)$$

where M_c is the molecular weight of carbon. We write

$$K_o = \frac{2M_c D_o}{RT} \left(\frac{T}{T_o}\right)^n \frac{Sh}{2r} \qquad (A5b)$$

eliminating $P\acute{o}_2$ from (A1) and (A5), we obtain for $\dot{R}_c$

$$\dot{R}_c = \frac{1}{2}\left\{\left(\frac{K_2K_o}{K_1} + K_o\ Po_2 + K_2\right) - \left[\left(\frac{K_2K_o}{K_1} + K_o\ Po_2 + K_2\right)^2 - 4\ K_2K_o\ Po_2\right]^{1/2}\right\} \qquad (A6)$$

where the choice of sign, in this solution of a quadratic equation, relates to the limit $K_o \to \infty$ for very fast diffusion.

Experiments on carbon, coal and coal char combustion can be used, with (A6), to define K_1 and K_2 as functions of temperature. Field, et al., 1967 present a summary of earlier studies by Tu, et al., 1934 and Golovina and Khaustovich, 1962. They conclude that all of the data for the rate of removal of carbon ($\dot{R}_c$ in our notation) in the temperature range 1000-1800°K can be represented adequately by a reaction rate which is first order in the partial pressure of oxygen and contains a single exponential with an activation energy of 35.7 kcal/mole. They note that in the higher temperature regime there is some evidence that the activation energy is less than this value.

Smith, 1971a, 1971b studied anthracites, semianthracites, petroleum coke and char from swelling bituminous coal, where the particles were less than 100 μ. It was observed that the anthracite, petroleum coke and char particles burned at constant density and that the activation energy was of the order of 20 kcal/mole. The semianthracite tended to burn at both decreasing density and size with approximately the same activation energy. It was assumed that the reactions were first order in oxygen partial pressure. Smith (1971a) noted that his data on anthracite and bituminous coal chars was consistent with the data of Field, 1969 and that his measurements for anthracite and semianthracite are consistent with

those of Field, 1970, and other investigators. Smith concluded that his measurements were in the pore diffusion controlled regime and that the apparent activation energy was therefore representative of desorption [c.f., Wheeler, 1951; Walker, et al., 1959].

The data of Field, 1969 were reexamined by Gray, et al., 1974; the Langmuir isotherm was used to represent the behavior of low rank char in a wide range of temperature. This representation involved adsorption control at high temperatures and desorption control at low temperatures.

We have noted the suggestion by Essenhigh and his coworkers that there is a contradiction in the assumption of a high activation energy (real or apparent) with a first order reaction rate. However, except for the data of Hamor, et al., 1973 on brown pulverized coal, most investigators have proposed such a representation of the reaction rate data. It may be, as suggested by Gray et al., 1974, that the range of oxygen partial pressures used in the experiments is not adequate to define precisely the order of the reaction. For the present we consider these relationships to be semiempirical and summarize the numerical constants in the Table (I) using the notation of (A1) and (A2); we also include Dobner's 1976 correlation for combustion of medium rank char.

For the temperatures appropriate to combustion in steam oxygen gasification processes ($\sim$1300°K) all of these correlations give approximately the same temperature dependence. The difference in activation energy is generally compensated for by the influence of the pre-exponential factor. Of course in a wide range of temperatures, the differences in activation energies would cause large variations in the reaction rates. For the present we expect to utilize the Langmuir isotherm with only a single Arrhenius expression as given by Field, 1969.

TABLE (I)

SUMMARY OF LANGMUIR ISOTHERM REPRESENTATION
OF CARBON, COAL AND CHAR COMBUSTION

Investigator	Particle Type (Size)	A_1 $\frac{gms}{cm^2\ sec\ atm}$	E_1 $\frac{kcal}{mole}$	A_2 $\frac{gms}{cm^2\ sec}$	E_2 $\frac{kcal}{mole}$
Field, et al., 1967	Carbon (1-2.54cm)	8710	35.7	∞	0
Smith, 1971a	Petroleum Coke (4-77μm)	20	18.2	∞	0
	Anthracite (42,72 μm)	10	16.7	∞	0
	Bituminous Char (34,64μm)	8	16.0	∞	0
Smith, 1971b	Semianthracite (6-78μm)	20.4	19.0	∞	0
Field, 1969	Low Rank Bituminous Char (28-105μm)	8710*	35.7	∞	0
Gray, et al., 1974	Low Rank Bituminous Char (Field, 1969)	1.6	6.0	1.27×10^3**	37.0
Dobner, 1976	Low-Medium Rank Char (Correlation)	60.0	20.4	∞	0

*T < 1300°K

**We've assumed an O_2 concentration of 10 percent.

With the choice of K_1 and K_2 in (A2) and the definition of transport velocity coefficient K_o in (A5) and (A6), the rate of carbon mass loss of a particle (A6) is defined. The nature of this mass loss shall, for the present, be assumed to be at constant particle density. While this is representative of some of the data [c.f., Avedesian and Davidson, 1973; Smith, 1971a; Field, et al., 1967, Nettleton, 1967], there is also evidence of mass loss at constant particle radius or at some combination of density and volume change [c.f., Field, et al., 1967]. At constant density the time rate of change of the particle radius is

$$-\rho^s \frac{dr}{dt} = \dot{R}_c \tag{A7}$$

This equation will be used to describe the evolution of particle size during combustion.

HETEROGENEOUS REACTION, PARTICLE-GAS HEAT TRANSFER

The Equations (A1) - (A7) define the mass flux and chemical reaction for a particle at temperature T' in an ambient gas flow of temperature T. It is necessary to introduce an energy balance for the particle to define the particle temperature. We assume that the temperature of the particle is uniform and write

$$\rho^s C_{p_c} \frac{dT'}{dt} = \frac{3\dot{R}_c}{rM_c}\left[C_{p_c}(T'-T_o) + C_{p_{o2}}(T'-T_o) - \frac{1}{2}\left\{C_{p_{co}}(T'-T_o] + \Delta H(0)\right\}\right] - \frac{3K_3}{r}(T'-T) - \frac{3\sigma\varepsilon}{r}\left\{(T')^4 - (T_\infty)^4\right\} \tag{A8}$$

where C_{p_i} is the specific heat at constant pressure for component i, $\Delta H(0)$ is the heat of formation of carbon monoxide at T_o, σ is the Stefan Boltzmann constant, T_∞ is a "wall" temperature and K_3 is the heat transfer coefficient

$$K_3 = \lambda_o \left(\frac{T}{T_o}\right)^m \frac{Nu}{2r} \tag{A9}$$

In this latter equation λ_o is the thermal diffusivity of the gas and the Nusselt number Nu is defined in terms of the Reynolds and Prandtl numbers by

$$Nu = 2 + \tilde{A}\, Re^{\tilde{B}}\, Pr^{\tilde{C}} \tag{A10}$$

where m, $\tilde{A}$, $\tilde{B}$, $\tilde{C}$ are constants analogous to the coefficients in (A3) and (A4). In both (A9) and in the earlier equation (A5b) we have used only the gas temperature in the free stream, T, to define the gas properties. These relationships can be further modified by introducing some mean temperature which accounts for the difference between that free stream temperature of the gas temperature at the surface of the particle, T´. Equations (A7) and (A8) must, in general, be solved simultaneously to define the particle radius r and the temperature of the particle T´ (and the reaction rate $\dot{R}_c$). For the case of diffusion control ($K_o << K_1, K_2$) the particle radius is independent of the particle temperature and may be directly obtained from (A7) with $\dot{R}_c \sim \frac{1}{r}$.

HOMOGENEOUS REACTIONS

The reactions R_2, R_3 and R_4 represent the chemistry of the gas phase surrounding the solid particle, where we write the reaction rates, in moles/cm^3 as Γ_i, i = 2, 3, 4. These reactions lead to differential changes in the gas composition which, without flow, would be expressed as

$$\frac{dC_{O_2}}{dt} = -\frac{1}{2}(\Gamma_2 + \Gamma_3)$$

$$\frac{dC_{CO}}{dt} = -(\Gamma_2 + \Gamma_4) \qquad \text{(A11)}$$

$$\frac{dC_{H_2}}{dt} = -\Gamma_3 + \Gamma_4$$

$$\frac{dC_{H_2O}}{dt} = \Gamma_3 - \Gamma_4$$

$$\frac{dC_{CO_2}}{dt} = \Gamma_2 - \Gamma_4$$

where C_i represents the mole of species i in a unit volume of gas.

The reaction rates Γ_i are, in general, functions of gas composition and temperature. Further, there is the possibility of catalytic influences because of the chemical composition of the solid particles. The oxidation of carbon monoxide through R_2 has been the subject of considerable investigation. We follow Field, et al., 1967 and use the semiempirical representation of Hottel, et al., 1965 to write

$$\Gamma_2 = 3 \times 10^{10} C_{Co} C_{O_2}^{0.3} C_{H_2O}^{0.5} \exp -\frac{16000}{RT} \qquad \text{(A12)}$$

The presence of C_{H_2O} in (A12) is indicative that this reaction is strongly influenced by the presence of water vapor. Field, et al. note that the equation can represent experimental results up to 1550°K and can likely be used at higher temperatures.

The actual kinetics of R3 are quite complicated [c.f., Penner, 1957; Lewis and Von Elbe, 1951]; however, the oxidation of hydrogen is a very fast reaction [c.f., Batchelder, et al., 1953], and we expect that it is in equilibrium for time scales of interest. That is, we can express the relationship between the molar concentrations of H_2, O_2 and H_2O as

$$\frac{C_{H_2O}}{C_{O_2} C_{H_2}^{1/2}} = K_{P,3}(RT)^{1/2} \tag{A13}$$

where $K_{P,3}$ is the equilibrium constant expressed in terms of partial pressures.

The water gas shift relationship is strongly influenced by iron catalysis. A relationship for this rate constant, based upon data for commercial iron catalysts, is presented in Blake, et al., 1976. This reaction rate is based upon a unit mass of catalyst. Let us assume that β is the fraction of the mass of char particles which is active within a volume of gas (defined by the radius of the weighting function used to derive our continuum balance equations, c.f., Blake, et al., 1976). This means that β is some function of the molecular mean free path, the surface and pore structure of the particles and the fraction of iron in the particle. Then the rate expression is

$$\Gamma_4 = \left\{4.03 \times 10^7 \exp - \frac{9692}{RT}\right\} \frac{\beta \rho^s T^2 \theta}{M_{CO} M_{H_2O}}$$

$$\left\{C_{Co} C_{H_2O} - \frac{M_{Co} M_{H_2O}}{M_{H_2} M_{Co_2}} \frac{1}{K_{P,4}} C_{H_2} C_{Co_2}\right\} \tag{A14}$$

The factor θ reflects the volume fraction of solid particles within the volume of space under consideration. For our present study we will likely use $\beta = .0035$ [c.f., Blake, et al., 1976], and we will ignore the presence of iron in our conservation of mass for the solid particle.

CONSERVATION EQUATIONS WITH CHEMICAL REACTIONS

The mass and energy relationships for the heterogeneous and homogeneous reactions of single char particles contribute to the conservation of mass and energy of a fluidized bed containing many such particles. We now use those relationships for single particles to derive the influence of chemical reactions on fluidized bed flows. Our basic assumptions are, first, the contribution of many particles is equal to a sum over the individual particles; second, the local space averaged gas phase properties represent the ambient gas conditions for the heterogeneous reactions; third, the homogeneous reactions are calculated with these space averaged gas properties and, finally, the particle temperature, T', is equal to the local space averaged solid temperature, T^s.

The conservation equations for fluidized beds are discussed in Blake, et al., 1976. We summarize these equations here, and present them in a slightly different form since we now wish to follow the time history of chemical species and the associated fluxes of mass and energy. The conservation of mass for the gas is represented by

$$\frac{\partial}{\partial t}\left[\rho_\alpha(1-\theta)\right] + \frac{\partial}{\partial x_i}\left[\rho_\alpha(1-\theta)\, v_i\right] = S_\alpha + (1-\theta)\Omega_\alpha \qquad \text{(A15)}$$

where this represents six equations for the species

$$\alpha = O_2,\ H_2O,\ H_2,\ CO,\ CO_2,\ N_2$$

For the solid phase we have

$$\frac{\partial \rho^s \theta}{\partial t} + \frac{\partial}{\partial x_i} \rho^s (1-\theta) u_i = - S_\beta \qquad \text{(A16)}$$

where

$$\beta = C$$

The quantities S_α represent interphase mass exchange while Ω_α represents species production from homogeneous reactions. For the present we regard N_2 as a diluent which does not participate in the reactions:

$$S_{N_2} = \Omega_{N_2} = 0 \ .$$

We thus consider six species for the gas and one species for the solid phase. Naturally, the influence of other species in the solid, such as ash, can be readily incorporated. The conservation of momentum equations for the gas and solid phases are, respectively

$$- \frac{\partial P}{\partial X_i} - \frac{B(\theta)}{(1-\theta)} (v_i - u_i) = 0 \qquad \text{(A17)}$$

$$\rho^s \left\{ \frac{\partial}{\partial t} (\theta u_i) + \frac{\partial}{\partial X_j} (\theta u_i u_j) \right\} = \frac{\partial P}{\partial X_i} + \frac{\partial \tau_{ij}}{\partial X_j} + \theta \rho^s g_i \qquad \text{(A18)}$$

We neglect both interphase momentum exchange and species diffusional influences on momentum conservation. The conservation of energy, neglecting viscous dissipation, can be written as

$$\frac{\partial}{\partial t}\left[\rho(1-\theta)e + \rho^s\theta e^s\right] + \frac{\partial}{\partial X_u}\left[\rho v_j(1-\theta)e + \rho^s u_j\theta e^s\right]$$

$$= -\frac{\partial}{\partial X_j}\left\{(1-\theta)\, q_i + \theta q_i^s\right\} \tag{A19}$$

where both e and q_i can include diffusional contributions. For the present we neglect such contributions. The specific internal energy of the gas is

$$e = \sum_\alpha \frac{\rho_\alpha}{\rho} e_\alpha = \sum_\alpha \frac{\rho_\alpha}{\rho}\left[C_{V_\alpha}\left\{T - T_o\right\}\right.$$

$$\left. + H_\alpha\,(0) - \Delta N_\alpha\, RT_o\right] \tag{A20}$$

where $H_\alpha(o)$ is the heat of formation of species α at T_o and ΔN_α is the change in moles when α is formed from the elements in their respective standard states [c.f., Penner, 1957]. The constitutive equations for P, τ_{ij}, e_α, e^s, q_i and q_i^s are

$$P = \sum_\alpha \frac{\rho_\alpha}{M_\alpha} RT = \sum_\alpha P_\alpha \tag{A21a}$$

$$\tau_{ij} = -\delta_{ij}\left\{P^s(\theta) + \lambda^s(\theta)\,\frac{\partial u_K}{\partial X_K}\right\}$$

$$+ \mu^s(\theta)\left\{\frac{\partial u_i}{\partial X_j} + \frac{\partial u_j}{\partial X_i} - \frac{2}{3}\,\delta_{ij}\,\frac{\partial u_K}{\partial X_K}\right\} \tag{A21b}$$

$$de_\alpha = C_{V_\alpha}\, dT \tag{A21c}$$

$$de^s = C_V^s\, dT^s \tag{A21d}$$

$$(1-\theta)\, q_i + \theta q_i^s = -\kappa(\theta)\, \frac{\partial T}{\partial X_i} \tag{A21e}$$

Further, the variation of particle radius and particle temperature requires that we adjoin to these equations the Lagrangian equations (A7) and (A8) where again we assume that the particle temperature T' is equal to the space averaged solid particle temperature T^s. The heterogeneous and homogeneous chemistry defines the source terms S_α, Ω_α for the species conservation in the gas phase; for S we use (A6), multiply by the weighting function $g|x_i - y_i|$ [Anderson and Jackson, 1967; Blake et al., 1976] and sum over all the particles to give for $\alpha = O_2$

$$S_{O_2} = -\sum_P \dot{R}_c\, 4\pi r^2\, \frac{M_{O_2}}{2M_c}\, g(|x_i - y_i|) \quad .$$

We note that the dependence of $\dot{R}_c$ is upon the local average field variables (e.g., T, T^s, $P_{O2} = \rho_{O2} \frac{RT}{M_{O2}}$) and the particle radius. Hence, if the particle radii are uniform within the radius of the weighting function, this integral is

$$S_{O_2} = -\frac{3\theta}{r}\, \frac{M_{O_2}\, \dot{R}_c}{2M_c} \tag{A22}$$

In a similar manner

$$S_{CO} = \frac{3\theta}{r}\, \frac{M_{CO}}{M_C}\, \dot{R}_c \tag{A23}$$

and for the solid phase $\beta = C$

$$S_C = - \frac{3\theta}{r} \dot{R}_C \tag{A24}$$

Since we have assumed that H_2O, CO_2 and H_2 do not react with the particle

$$S_{CO_2} = S_{H_2O} = S_{H_2} = 0 \tag{A25}$$

The homogeneous reactions determine the source terms Ω_α. These homogeneous reactions are defined by (A10) - (A13). We write

$$\begin{aligned}
(1-\theta)\ \Omega_{O_2} &= - \frac{(1-\theta)M_{O_2}}{2} \left\{\Gamma_2 + \Gamma_3\right\} \\
(1-\theta)\ \Omega_{CO} &= - (1-\theta)M_{CO} \left\{\Gamma_2 + \Gamma_4\right\} \\
(1-\theta)\ \Omega_{H_2} &= (1-\theta)M_{H_2} \left\{- \Gamma_3 + \Gamma_4\right\} \\
(1-\theta)\Omega_{H_2O} &= (1-\theta)\ M_{H_2O} \left\{\Gamma_3 - \Gamma_4\right\} \\
(1-\theta)\Omega_{CO_2} &= (1-\theta)M_{CO_2} \left\{\Gamma_2 - \Gamma_4\right\}
\end{aligned} \tag{A26}$$

Noting that Γ_i can be expressed in terms of ρ_i we have with (A7), (A8) and (A20) - (A26)a system of equations for ρ_{02}, ρ_{CO}, ρ_{H_2}, ρ_{H_2O}, ρ_{CO_2}, ρ_{N_2}, u_i, v_i, T^s, T, r, θ.

APPENDIX B
PARAMETRIC CALCULATIONS FOR FLUIDIZED BEDS

The two dimensional computer model of fluidized beds was applied in the first year of the contract to investigate the influence of mass flow rate in a shallow bed with a specific distributor plate having discrete injection points [Blake, et al., 1976]. Bubble formation and bubble motion in the bed was examined for a range of mass flow rates between the condition of a spouted bed and that wherein the rising bubble became vanishingly small.

In order to evaluate the code, preparatory to some calculations of specific reactor configurations we have continued to exercise the numerical model in various parametric studies. These calculations are illustrative of the ability of the code to treat different fluidized bed environments. Further, we have exercised the numerical procedures such as the definition of zonal dimensions, e.g., we have used zones with aspect ratios different from unity, to study the influence of numerical artifacts upon the calculations.

We have mentioned the earlier parametric calculations wherein a distributor plate with discrete injection points was examined. To examine the flow field associated with a more continuous injection of mass, we have studied configurations such as the two-dimensional planar bed shown in Figure B1. There are two aspects to this calculation which are of interest. First, there is the nature of the continuous inlet flow distributions wherein the inlet velocity is a maximum at the center line of the bed and linearly decreases to zone at the outer wall. Second, we wished to illustrate the ability of the code to treat an extreme flow condition wherein the superficial velocities (if the mass flow was uniformly distributed) was twice that for minimum fluidization.

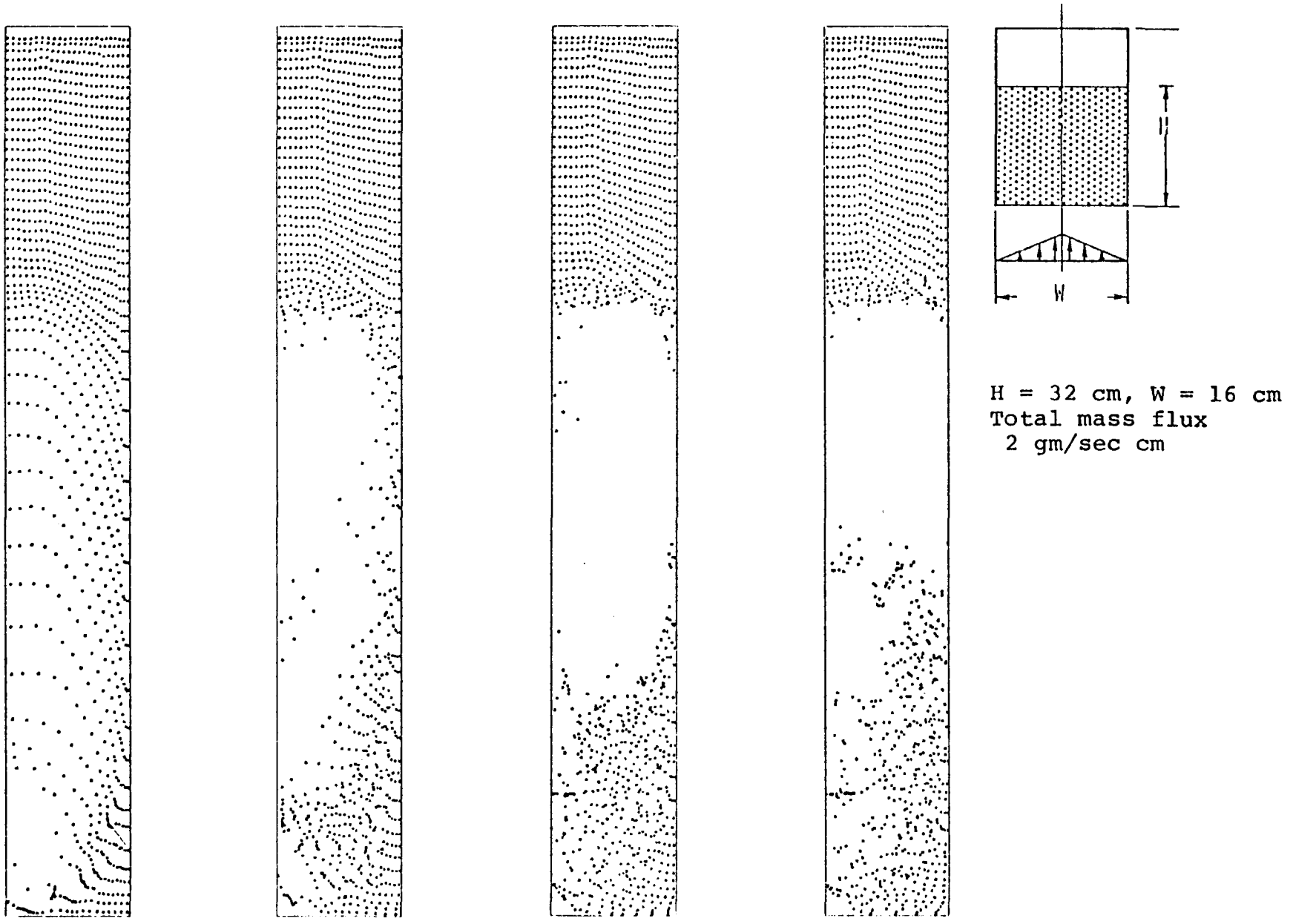

Figure B1. Particle distributions in planar fluidized bed, one half of bed shown, superficial velocity greater than minimum fluidization velocity.

The bed expands rapidly and, because the boundary conditions on particle velocity at the top of the bed, did not permit the particles to leave the bed, these particles are suspended at the top of the free board region for $T \leq 0.9$ sec. The flow tends to be a maximum near the centerline of the bed and hence while particles can fall at the outer edge of the bed ($T = 0.6$ to $T = 0.9$ sec) they are elutriated and carried upwards in the center. For the same mass flow rate, but with the hydrostatic pressure in the bed doubled, the corresponding particle motion is shown in Figure B2. The bed does not expand as vigourously as in Figure B1 and further, the expanded bed subsequently collapses and tends to operate as a surging bed. Of course, by doubling the hydrostatic pressure we approximately double the density and for a constant mass flow rate we are essentially decreasing, by a factor of two, the superficial velocity. This has a major influence upon the relative behavior of the beds in Figures B1 and B2.

Again, the calculations in Figures B1 and B2 are illustrative of parametric tests using the fluidized bed computer model. Other calculations included the influences of bed height to width ratio and mass flow rate with both discrete and continuous injection of gas.

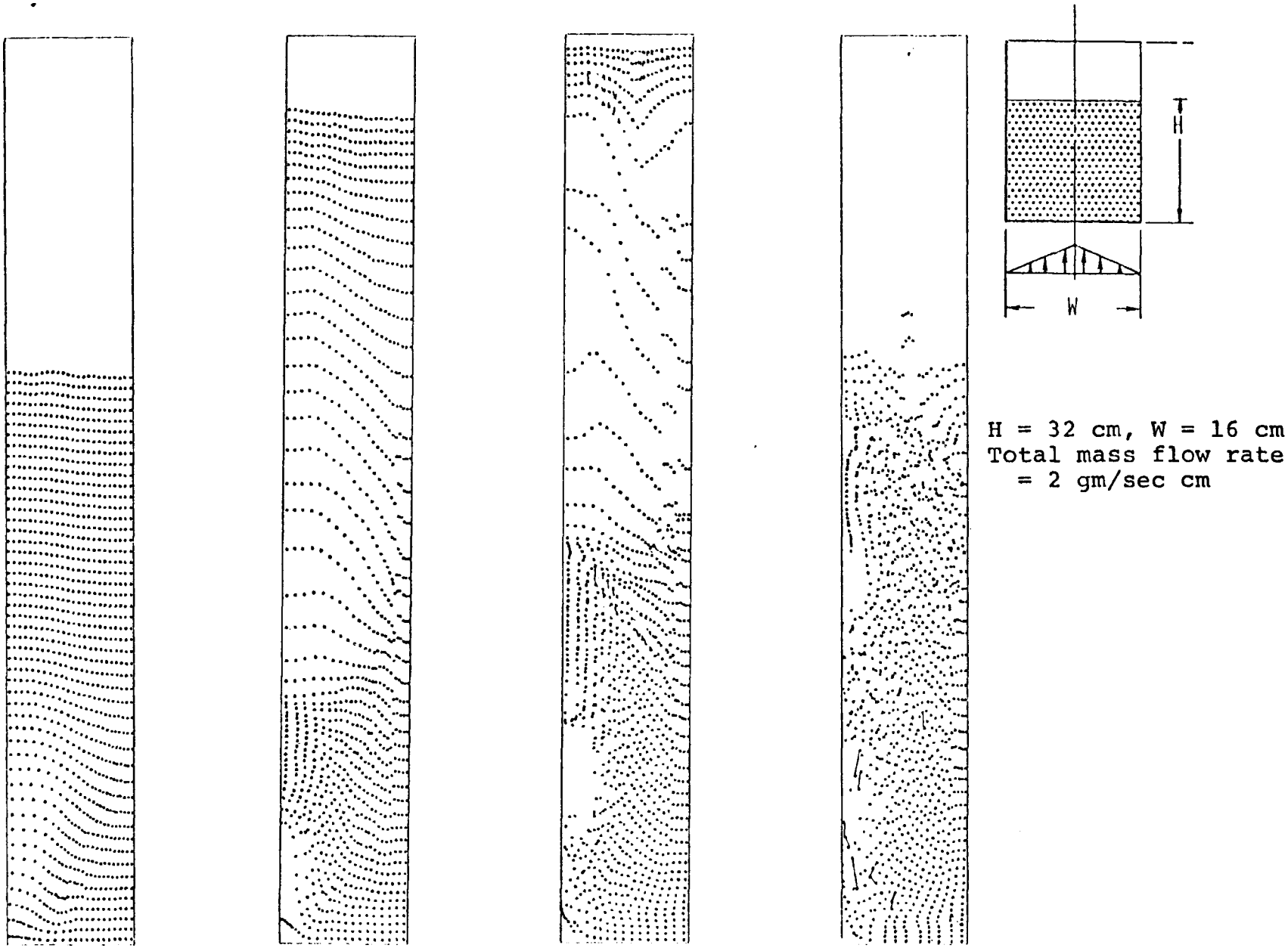

Figure B2. Particle distribution in planar fluidized bed, one half of bed showing, high pressure.

APPENDIX C

DERIVATION OF EQUATIONS FOR TURBULENT ENTRAINED FLOWS

In Blake [1976] a derivation of the conservation equations for the solid particle-gas flows appropriate to entrained processes was presented. In this Appendix, we recast the basic equations somewhat, formulate the time-averaged turbulent version of these equations along with the thermodynamic and caloric equations of state needed for mathematical closure, indicate the assumptions involved in the derivation of the turbulent version of these equations, and, finally, give an order of magnitude estimate of the errors inherent in some of these assumptions. A derivation of the conservation equations for a number of turbulence quantities (i.e., turbulence kinetic energy, turbulence dissipation rate, etc.) needed to provide the turbulence closure will be left to future reports as will the explicit formulation of boundary conditions and the form of the chemical reaction and radiation terms.

In our present study, we consider conservation equations which include several general order-of-magnitude approximations. Specifically, we have:

1. Ignored terms with <u>laminar</u> transport coefficients. We anticipate that they will be dwarfed in magnitude by identical terms with <u>turbulent</u> transport coefficients arising in the course of our derivation of the gaseous turbulent mean conservation equations. The particle-gas interaction terms are unaffected by this rule however.

2. Ignored the momentum and kinetic energy exchange accompanying interphase mass exchange because we expect them to be quite small in comparison with the local momentum and kinetic energy of either phase.

3. Ignored the thermalization of kinetic energy due to interphase drag since it is expected to be a negligible influence on temperature compared to chemical reaction and/or interphase heat transfer.

Let us now write the conservation equations for the instantaneous (as contrasted with the time averaged) flow field. We have:

$$\frac{\partial \rho_f}{\partial t} + \frac{\partial (\rho_f v_i)}{\partial x_i} = S \quad \text{where} \quad \rho_f \equiv \rho\phi, \tag{C.1}$$

S = rate of <u>increase</u> of ρ_f due to solid mass being gasified by chemical reaction.

<u>Total Solid Mass</u>

$$\frac{\partial \rho_p}{\partial t} + \frac{\partial (\rho_p u_i)}{\partial x_i} = - S \quad \text{where} \quad \rho_p = \rho_s(1-\phi) \tag{C.2}$$

<u>Total Gas Momentum</u>

$$\frac{\partial (\rho_f v_i)}{\partial t} + \frac{\partial (\rho_f v_i v_j)}{\partial x_j} = - \frac{\partial P}{\partial x_i} - G(\mu_\ell, r)\ \rho_p (v_i - u_i) + \rho_f g_i \tag{C.3}$$

where $G(\mu_\ell, r)$ = Stokes' Flow coefficient for total particle-gas drag as a function of μ_ℓ = gas laminar dynamic viscosity and r = particle radius.

<u>Total Solid Momentum</u>

$$\frac{\partial (\rho_p u_i)}{\partial t} + \frac{\partial (\rho_p u_i u_j)}{\partial x_j} = G(\mu_\ell, r)\ \rho_p (v_i - u_i) + \rho_p g_i \tag{C.4}$$

Gaseous Species Mass

$$\frac{\partial(\rho_f F_\alpha)}{\partial t} + \frac{\partial(\rho_f F_\alpha v_i)}{\partial x_i} = S_\alpha + \Omega_{f,\alpha} \qquad (C.5)$$

where F_α = mass fraction of species in gas and $\Omega_{f,\alpha} (= \phi\Omega_\alpha)$ and S_α = rate of increase in $\rho_{f,\alpha} = \rho_f F_\alpha$ due to creation of species α via gas-phase chemical reaction and solid mass gasification, respectively. Note that $\sum_\alpha S_\alpha = S$ and $\sum_\alpha \Omega_{f,\alpha} = 0$.

Gas Internal Energy

$$\frac{\partial(\rho_f e_f)}{\partial t} + \frac{\partial(\rho_f e_f v_i)}{\partial x_i} = - P \frac{\partial v_i}{\partial x_i} + \sum_\alpha S_\alpha h_\alpha(T_p) - H(K_\ell, r)(T_f - T_p) - \frac{\partial q_i}{\partial x_i} \qquad (C.6)$$

where

e_f = Specific internal energy of gas phase including energy of formation.

q_i = Heat flux vector in gas phase which may include conduction, species diffusion, and radiation effects.

T_f = Gas phase temperature.

$h_\alpha(T_p)$ = Specific enthalpy of species α at solid phase temperature, T_p, including heat of formation.

$H(K_\ell, r)$ = Stokes' Flow coefficient for particle-gas heat transfer.

K_ℓ = Laminar gas conductivity.

Solid Internal Energy

$$\frac{\partial(\rho_p e_p)}{\partial t} + \frac{\partial(\rho_p e_p u_i)}{\partial x_i} = -\sum_\alpha S_\alpha h_\alpha(T_p)$$

$$+ H(K_\ell, r)(T_f - T_p) - \frac{\partial q_{pi}}{\partial x_i} \qquad \text{(C.7)}$$

where

e_p = Specific internal energy for solid phase, including energy of formation (usually zero).

q_{pi} = Heat flux vector in solid phase.

Gaseous Thermodynamic Equation of State

$$P = \rho RT \sum_\alpha \frac{F_\alpha}{M_\alpha} \qquad \text{(C.8)}$$

where

R = Universal molar gas constant .

M_α = Molecular weight of species α.

Gaseous Caloric Equation of State

$$\rho_f e_f = \rho_f \sum_\alpha F_\alpha e_\alpha(T_f) = \rho_f \sum_\alpha F_\alpha \left\{ e_\alpha(T_0) + \int_{T_0}^{T_f} C_{v,\alpha}(T)\, dT \right\} \qquad \text{(C.9)}$$

where $e_\alpha(T)$ = specific internal energy of species α at temperature, T, including energy of formation; T_0 = 298.15°K is the reference temperature at which energy of formation data is available; and $C_{v,\alpha}$ is the (mass not molar) specific heat at constant volume of species α at temperature, T.

Solid Caloric Equation of State

$$\rho_p e_p = \rho_p e_p(T_0) + \rho_p \int_{T_0}^{T_p} C_{v,p}(T)\, dT \qquad (C.10)$$

where $e_p(T_0)$ = specific internal energy of solid particle at reference temperature and $C_{v,p}(T)$ = (mass) specific heat at constant volume of particle at temperature, T.

In addition to the previous ten equations, we have three definitions to which we have referred that are needed to mathematically close the system, viz.,

Definitions

$$\sum_{\alpha} \rho_{f,\alpha} = \rho_f \quad \text{or} \quad \sum_{\alpha} F_{\alpha} = 1 \qquad (C.11)$$

$$\rho_f = \rho\phi \qquad (C.12)$$

$$\phi = 1 - \frac{\rho_p}{\rho_s} \qquad (C.13)$$

The above equations constitute a set of 16+N (N = number of gaseous phase chemical species considered) equations with only 15+N unknowns. As is standard, one of the gaseous species equations must be discarded since summing the N versions of Eqs. (C.5) and using Eq. (C.11) yields Eq. (C.1) (i.e., the sum of the gaseous species mass conservation equations is redundant with respect to the overall gaseous mass conservation equation). This reduces our equation set to 15+N so our system is mathematically closed.

We shall be interested, initially, at least, in examining the case of locally isothermal conditions (i.e., $T_p = T_f = T$). For that case we can combine Eq. (C.6) and (C.7) into

a total internal energy equation. Such action, which will be exhibited below when we consider the turbulent form of the equations, reduces our set to 14+N equations with 14+N unknowns.

The above equations constitute a closed mathematical set for the instantaneous quantities, but this is not too useful for characterizing turbulent systems wherein the time-averaged quantities are more easily observable and considerably more significant.

Let us now turn to the time-averaged form of Eqs. (C.1)-(C.13) and how we currently intend to deal with them. We shall take each equation separately and, thus, build up a set of calculational variables.

Taking the time average of Eq. (C.1), we get:

$$\frac{\partial \overline{\rho}_f}{\partial t} + \frac{\partial (\overline{\rho_f v_i})}{\partial x_i} = \overline{S} \qquad \text{(C.11a)}$$

where $(\bar{\ })$ denotes the time-average of a quantity which, theoretically at least, is taken over times large with respect to the time scales of the turbulent fluctuations, but short with respect to the time scales of interest in the calculations. Note that we have only formally time-averaged the chemistry term; we shall not go any further at this time. Now, traditionally we have broken every instantaneous quantity, β, into a time-averaged part, $\overline{\beta}$, and the instantaneous fluctuation from $\overline{\beta}$, $\beta' \equiv \beta - \overline{\beta}$, so that $\overline{\beta'} \equiv 0$. For constant density flows, this approach is satisfactory [Launder and Spalding, 1972], but it leads to major problems in flows with large density variations such as those involved with combustion [Kent and Bilger, 1973]. Consequently, we have chosen to use a variation of Favre averaging in which if ρ is a density, we have $\beta \equiv \tilde{\beta} + \beta''$

and $\overline{\rho\beta} \equiv \overline{\rho}\tilde{\beta}$ so that $\overline{\rho\beta''} = 0$ but $\overline{\beta''} \neq 0$. Thus, we define $v_i \equiv \tilde{v}_i + v''$ and take $\overline{\rho_f v_i} = \overline{\rho}_f \tilde{v}_i$ so $\overline{\rho_f v_i''} = 0$. This yields:

$$\frac{\partial \overline{\rho}_f}{\partial t} + \frac{\partial (\overline{\rho}_f \tilde{v}_i)}{\partial x_i} = \overline{S} \qquad \text{(C.1b)}$$

Taking time-averages of Eq. (C.2) yields:

$$\frac{\partial \overline{\rho}_p}{\partial t} + \frac{\partial (\overline{\rho_p u_i})}{\partial x_i} = - \overline{S} \qquad \text{(C.2a)}$$

Now, defining $u_i \equiv \tilde{u}_i + u_i''$ with

$\overline{\rho_p u_i} = \overline{\rho}_p \tilde{u}_i$ so $\overline{\rho_p u_i''} = 0$, we get:

$$\frac{\partial \overline{\rho}_p}{\partial t} + \frac{\partial (\overline{\rho}_p \tilde{u}_i)}{\partial x_i} = - \overline{S} \qquad \text{(C.2b)}$$

Averaging Eq. (C.3) over time and ignoring any fluctuations in $G(\mu_\ell, r)$, we get:

$$\frac{\partial (\overline{\rho_f v_i})}{\partial t} + \frac{\partial (\overline{\rho_f v_i v_j})}{\partial x_j} = - \frac{\partial \overline{P}}{\partial x_i} - G(\mu_\ell, r)\ \overline{\rho_p (v_i - u_i)} + \overline{\rho}_f g_i \qquad \text{(C.3a)}$$

The $\overline{\rho_f v_i}$ and $\overline{\rho_p u_i}$ terms were treated above, so let us turn to the others. We have

$$\overline{\rho_f v_i v_j} = \overline{\rho_f (\tilde{v}_i + \tilde{v}_i'')(v_j + v_j'')} = \overline{\rho}_f \tilde{v}_i \tilde{v}_j + [\tilde{v}_i \overline{(\rho_f v_j'')} + \tilde{v}_j \overline{(\rho_f v_i'')}]$$

$$+ \overline{\rho_f v_i'' v_j''},$$

but we saw that

$$\overline{\rho_f v_i''} = \overline{\rho_f v_j''} \equiv 0,$$

so we have

$$\overline{\rho_f v_i v_j} = \bar{\rho}_f \tilde{v}_i \tilde{v}_j + \overline{\rho_f v_i'' v_j''}.$$

The $\overline{\rho_p v_i}$ term is a troublesome one since it represents the interaction of the weighted particle density (i.e., $\rho_p = \rho_s (1-\phi)$) with gas velocity. Now

$$\overline{\rho_p v_i} = \bar{\rho}_p \tilde{v}_i + \overline{\rho_p v_i''} = \bar{\rho}_p \tilde{v}_i + \overline{\rho_p v_i''} - \overline{\rho_f v_i''} = \bar{\rho}_p \tilde{v}_i + \overline{(\rho_p - \rho_f) v_i''}$$

since

$$\overline{\rho_f v_i''} = 0$$

so the troublesome term can be thought of as either $\overline{\rho_p v_i''}$ or $\overline{(\rho_p - \rho_f) v_i''}$.

While one may argue that turbulent variations in solid quantities (e.g., ρ_p, u_i, etc.) may be only weakly correlated with those in gaseous quantities, we do not believe that such a principle is sufficiently well validated at this time, either qualitatively or quantitatively, to justify ignoring $\overline{\rho_p v_i''}$. Nevertheless, while we have not been able to prove, or even satisfactorily justify, the dropping of the $\overline{\rho_p v_i''}$ term, we shall do so for convenience sake, at least on an interim basis. Work shall continue on trying to either justify its omission or properly model it. Applying these rules, Eq. (C.3a) becomes:

$$\frac{\partial(\bar{\rho}_f\tilde{v}_i)}{\partial t} + \frac{\partial(\bar{\rho}_f\tilde{v}_i\tilde{v}_j)}{\partial x_j} = -\frac{\partial\bar{P}}{\partial x_i} - G(\mu_\ell,r)\ \bar{\rho}_p(\tilde{v}_i-\tilde{u}_i) + \bar{\rho}_f g_i$$

$$- \frac{\partial(\overline{\rho_f v_i'' v_j''})}{\partial x_j} \qquad \text{(C.3b)}$$

where the last term will be seen to be the divergence of the turbulent stress.

Treating Eq. (C.4) analogously to (C.3), we get for the time-averaged form:

$$\frac{\partial(\overline{\rho_p u_i})}{\partial t} + \frac{\partial(\overline{\rho_p u_i u_j})}{\partial x_j} = G(\mu_\ell,r)\ \overline{\rho_p(v_i-u_i)} + \bar{\rho}_p g_i \qquad \text{(C.4a)}$$

which becomes

$$\frac{\partial(\bar{\rho}_p\tilde{u}_i)}{\partial t} + \frac{\partial(\bar{\rho}_p\tilde{u}_i\tilde{u}_j)}{\partial x_j} = G(\mu_\ell,r)\ \bar{\rho}_p(\tilde{v}_i-\tilde{u}_i) - \frac{\partial(\overline{\rho_p u_i'' u_j''})}{\partial x_j}$$

$$+ \bar{\rho}_p g_i \qquad \text{(C.4b)}$$

Time-averaging Eq. (C.5) yields:

$$\frac{\partial(\overline{\rho_f F_\alpha})}{\partial t} + \frac{\partial(\overline{\rho_f F_\alpha v_i})}{\partial x_i} = \bar{S}_\alpha + \bar{\Omega}_{f,\alpha} \qquad \text{(C.5a)}$$

Now, define $F_\alpha \equiv \tilde{F}_\alpha + F_\alpha''$ such that $\overline{\rho_f F_\alpha} \equiv \bar{\rho}_f\tilde{F}_\alpha$ or $\overline{\rho_f F_\alpha''} = 0$. We get:

$$\frac{\partial(\bar{\rho}_f\tilde{F}_\alpha)}{\partial t} + \frac{\partial(\bar{\rho}_f\tilde{F}_\alpha\tilde{v}_i)}{\partial x_i} = \bar{S}_\alpha + \bar{\Omega}_{f,\alpha} - \frac{\partial(\overline{\rho_f F_\alpha'' v_i''})}{\partial x_i} \qquad \text{(C.5b)}$$

where the last term will be seen to be the divergence of the turbulent species mass diffusion flux vector.

As mentioned above, if we assume a local thermodynamic equilibrium, there will only be one temperature for both gas and solid. Thus, Eqs. (C.6), (C.7), (C.9) and (C.10) are related in that we have four equations for the three unknowns: e_p, e_f and T. Thus, before continuing, let us add Eqs. (C.6) and (C.7) to yield:

$$\frac{\partial(\rho_f e_f+\rho_p e_p)}{\partial t} + \frac{\partial(\rho_f e_f v_i+\rho_p e_p u_i)}{\partial x_i} = - p \frac{\partial v_i}{\partial x_i} - \frac{\partial(q_i+q_{p_i})}{\partial x_i} \qquad (C.14)$$

Taking time-averages of Eq. (C.14) results in:

$$\frac{\partial(\overline{\rho_f e_f}+\overline{\rho_p e_p})}{\partial t} + \frac{\partial(\overline{\rho_f e_f v_i}+\overline{\rho_p e_p u_i})}{\partial x_i} = - \overline{p \frac{\partial v_i}{\partial x_i}} - \frac{\partial(\bar{q}_i+\bar{q}_{p_i})}{\partial x_i} \qquad (C.14a)$$

Let us now take time-averages of Eqs. (C.9) and (C.10) to get:

$$\overline{\rho_f e_f} = \sum_\alpha \overline{\rho_f F_\alpha e_\alpha(T)} = \sum_\alpha \overline{\rho_f F_\alpha \left\{ e_\alpha(T_0) + \int_{T_0}^{T} C_{v,\alpha}(T)dT \right\}}$$

$$= \sum_\alpha \left\{ \overline{\rho_f F_\alpha} e_\alpha(T_0) + \overline{\rho_f F_\alpha \int_{T_0}^{T} C_{v,\alpha}(T)dt} \right\} \qquad (C.9a)$$

and

$$\overline{\rho_p e_p} = \bar{\rho}_p e_p(T_0) + \overline{\rho_p \int_{T_0}^{T} C_{v,p}(T)dt} \qquad (C.10a)$$

Now define $T \equiv \tilde{T} + T''$; we will not yet specify the division between $\tilde{T}$ and T'' except that T'' is affected by the time-

averaging process while $\tilde{T}$ is not. Let us now add Eqs. (C.9a) and (C.10a) together and substitute for T, which yields:

$$\overline{\rho_p e_p} + \overline{\rho_f e_f} = \bar{\rho}_p \left\{ e_p(T_0) + \int_{T_0}^{\tilde{T}} C_{v,p}(T)\,dT \right\}$$

$$+ \sum_\alpha \bar{\rho}_f \tilde{F}_\alpha \left\{ e_\alpha(T_0) + \int_{T_0}^{\tilde{T}} C_{v,\alpha}(T)\,dT \right\}$$

$$+ \overline{\int_{\tilde{T}}^{\tilde{T}+T''} \left\{ \rho_p C_{v,p}(T) + \sum_\alpha \rho_f F_\alpha C_{v,\alpha}(T) \right\} dT} \qquad \text{(C.15)}$$

Now, the first { }'d term is $e_p(\tilde{T})$ including the solid energy of formation, $e_p(T_0)$; the second { }'d term is $e_\alpha(\tilde{T})$ including the energy of formation of species α, $e_\alpha(T_0)$; while the last term in { } is the instantaneous <u>mixture</u> constant volume specific heat per unit volume, $C_{v,m}$, which is a function of both temperature and time. Thus, we can write Eq. (C.15) as:

$$\overline{\rho_p e_p} + \overline{\rho_f e_f} = \bar{\rho}_p e_p(\tilde{T}) + \bar{\rho}_f \sum_\alpha \tilde{F}_\alpha e_\alpha(\tilde{T})$$

$$+ \overline{\int_{\tilde{T}}^{\tilde{T}+T''} C_{v,m}(T,t)\,dT} \qquad \text{(C.15a)}$$

If we now define the split between $\tilde{T}$ and T'' such that the last term in Eq. (C.15a) vanishes, we get:

$$\overline{\rho_p e_p} + \overline{\rho_f e_f} = \bar{\rho}_p e_p(\tilde{T}) + \sum_\alpha \bar{\rho}_f \tilde{F}_\alpha e_\alpha(\tilde{T}) \qquad \text{(C.15b)}$$

We might note at this point that the above definition of $\tilde{T}$, T'' corresponds to a choice of $\tilde{T}$ such that the instantaneous variations in T about $\tilde{T}$ (i.e., T'') result in exactly as much (excess) mixture internal energy (per unit volume) existing in the excursions above $\tilde{T}$ as (deficit) mixture internal energy exists in the excursions below $\tilde{T}$ when averaged over the time scale used for averaging turbulent fluctuations. As such, it differs from the conventional $\bar{T}$ which is based on temperature itself instead of mixture internal energy or another possible definition wherein pressure is used instead of temperature or mixture internal energy. That latter definition would be most convenient for use in simplifying the turbulent form of the thermodynamic equation of state (Eq. (C.8)), but because of the differences between such temperature definitions, one is forced to choose one and accept the inconveniences and/or errors that choice imposes. We have made our choice and will demonstrate below its consequences.

Just as our definition of $\tilde{T}$, T'' has a more complicated form than our previous definitions (e.g., $\tilde{v}_i$, v_i'', etc.), the implications of that definition are also less obvious. Let us define the following quantities:

$$\tilde{e}_p \equiv e_p(\tilde{T}), \quad e_p'' \equiv \int_{\tilde{T}}^{\tilde{T}+T''} C_{v,p}(T)\,dT$$

so

$$e_p = \tilde{e}_p + e_p''$$

and

$$\tilde{e}_f \equiv \sum_\alpha \tilde{F}_\alpha e_\alpha(\tilde{T}), \quad e_f'' \equiv \sum_\alpha F_\alpha \int_{\tilde{T}}^{\tilde{T}+T''} C_{v,\alpha}(T)\,dT \qquad (C.16)$$

so

$$e_f = \tilde{e}_f + e_f''$$

Then our definition of $\tilde{T}$, T'' implies that $\overline{\rho_p e_p'' + \rho_f e_f''} = 0$, but it says nothing about $\overline{\rho_p e_p''}$ or $\overline{\rho_f e_f''}$ separately. Consequently, we have a rather unusual term appearing in the resultant turbulent expression for advection of internal energy. That is

$$\overline{\rho_f e_f v_i} + \overline{\rho_p e_p u_i} = \left(\bar{\rho}_f \tilde{e}_f \tilde{v}_i + \bar{\rho}_p \tilde{e}_p \tilde{u}_i\right) + \left(\overline{\rho_f e_f'' v_i''} + \overline{\rho_p e_p'' u_i''}\right)$$

$$+\left(\overline{\rho_f e_f''}\tilde{v}_i + \overline{\rho_p e_p''}\tilde{u}_i\right) \qquad (C.17)$$

A comparison with the terms appearing in Eqs. (C.3)-(C.5) shows that besides the mean advection and turbulent diffusion terms whose analogues appear in Eq. (C.17), we have the third ()'d term in Eq. (C.17) which has no analogue in Eqs. (C.3)-(C.5). This term can be written alternatively as

$$\overline{\rho_f e_f''}\tilde{v}_i + \overline{\rho_p e_p''}\tilde{u}_i = \overline{\rho_f e_f''}\,(\tilde{v}_i - \tilde{u}_i) = \overline{\rho_p e_p''}\,(\tilde{u}_i - \tilde{v}_i) \qquad (C.18)$$

and represents the net convection of turbulent mixture internal energy by the mean velocities. At this point we have no way to model such terms so we will arbitrarily drop them, at least temporarily.

The last term in Eq. (C.14) to be considered is the $\overline{P\ \partial v_i/\partial x_i}$ term. This can be written as

$$\overline{P \frac{\partial v_i}{\partial x_i}} = \bar{P} \frac{\partial \tilde{v}_i}{\partial x_i} + \overline{P \frac{\partial v_i''}{\partial x_i}} \qquad \text{(C.19)}$$

The $P\ \partial v_i/\partial x_i$ term represents the only kinetic-internal energy conversion mechanism remaining in the energy equation. Since "one BTU is worth many ft-lbf", it is possible that this pressure-work effect may also prove negligible in comparison to chemical reaction effects, but the large gas density changes induced by combustion and the possibly high operating pressures envisioned for entrained gasifiers/combustors makes the validity of such a simplification somewhat unsure. Thus, our approach is to discard the second term in Eq. (C.19) while retaining and monitoring, at least temporarily, the first term as an order-of-magnitude indicator of the significance of the pressure-work term. In this manner, we can let our calculational experience dictate the ultimate retention or omission of this term.

Combining all of the above derivations and decisions, the energy related equations (Eqs. (C.6), (C.7), (C.9), and (C.10)) reduce to the following three relationships:

$$\frac{\partial (\bar{\rho}_f \tilde{e}_f + \bar{\rho}_p \tilde{e}_p)}{\partial t} + \frac{\partial (\bar{\rho}_f \tilde{e}_f \tilde{v}_i + \bar{\rho}_p \tilde{e}_p \tilde{u}_i)}{\partial x_i} = - \bar{P} \frac{\partial \tilde{v}_i}{\partial x_i} \qquad \text{(C.14b)}$$

$$- \overline{\frac{\partial (\rho_f e_f'' v_i'' + \rho_p e_p'' u_i'')}{\partial x_i}} - \frac{\partial (\bar{q}_i + \bar{q}_{p_i})}{\partial x_i}$$

where the second term on the R.H.S. will be seen to be the divergence of the turbulent internal energy diffusion flux vector;

$$\overline{\rho_f e_f} = \bar{\rho}_f \tilde{e}_f = \bar{\rho}_f \sum_\alpha \tilde{F}_\alpha e_\alpha(\tilde{T})$$

$$= \bar{\rho}_f \sum_\alpha \tilde{F}_\alpha \left\{ e_\alpha(T_0) + \int_{T_0}^{\tilde{T}} C_{v,\alpha}(T)\,dT \right\} \qquad \text{(C.9b)}$$

and

$$\overline{\rho_p e_p} = \bar{\rho}_p \tilde{e}_p = \bar{\rho}_p e_p(\tilde{T}) = \bar{\rho}_p \left\{ e_p(T_0) + \int_{T_0}^{\tilde{T}} C_{v,p}(T)\,dT \right\} \qquad \text{(C.10b)}$$

Now, let us turn our attention to Eqs. (C.8), (C.11)-(C.13). Taking time-averages of Eq. (C.11) after substituting $\rho_{f,\alpha} = \rho_f F_\alpha$, we get

$$\sum_\alpha \overline{\rho_f F_\alpha} = \sum_\alpha \bar{\rho}_f \tilde{F}_\alpha = \bar{\rho}_f \quad \text{or} \quad \sum_\alpha \tilde{F}_\alpha = 1, \qquad \text{(C.11a)}$$

but

$$\sum_\alpha F_\alpha = \sum_\alpha (\tilde{F}_\alpha + F''_\alpha) = 1 \quad \text{so} \quad \sum_\alpha F''_\alpha \equiv 0.$$

Time-averages of Eq. (C.13) yields

$$\bar{\phi} = 1 - \frac{\bar{\rho}_p}{\rho_s} \qquad \text{(C.13a)}$$

A time-average of Eq. (C.12) yields:

$$\overline{\rho_f} = \overline{\rho\phi} = \overline{\rho}\ \overline{\phi} + \overline{\rho'\phi'} \simeq \overline{\rho}\ \overline{\phi} \quad (\text{i.e., } \overline{\rho'\phi'} \simeq 0) \qquad (C.12a)$$

There are two arguments why the above approximation is probably valid:

1. ρ' is primarily due to the "interchange" of hot and cold (i.e., burned and unburned) parcels of gas due to turbulent motion while ϕ' is primarily due to turbulence induced changes in the particle number density. These dissimilar physical phenomena are unlikely to be closely correlated and since both have zero means, their joint mean is also likely to approximate zero.

2. The density ratio of unburned to burned gas is about 10 or less while ϕ is expected to vary by only a few percent from 1.0 due to the light solid loading anticipated in entrained gasifiers. Thus,

$$\left|\frac{\rho'}{\overline{\rho}}\right|\left|\frac{\phi'}{\overline{\phi}}\right| \leq O(10\times10^{12}) = O(10^{-1})$$

as an upper bound, especially insofar as we have assumed perfect time-correlation (see 1). Thus, we feel that the approximation shown in Eq. (C.12a) is justified and will use it. We guess the true error to be of order 1 percent.

Equations (C.12a) and (C.13a) serve to define $\overline{\rho}$ and $\overline{\phi}$, given $\overline{\rho}_f$ and $\overline{\rho}_p$. We now proceed to Eq. (C.8), a time-average of which yields:

$$\overline{P} = \sum_{\alpha} \frac{R}{M_\alpha} \overline{\rho T F_\alpha} \approx \sum_{\alpha} \frac{R}{M_\alpha \overline{\phi}} \overline{\rho_f T F_\alpha} = \frac{R}{\overline{\phi}} \sum_{\alpha} \frac{\overline{\rho_f F_\alpha T}}{M_\alpha}$$

$$= \frac{R}{\overline{\phi}} \sum_{\alpha} \left(\frac{\overline{\rho}_f \tilde{F}_\alpha \tilde{T}}{M_\alpha} + \frac{\overline{\rho_f F_\alpha T''}}{M_\alpha} \right) \qquad \text{(C.8a)}$$

where the indicated approximation is good to a couple percent since that is the order of difference between ρ and ρ_f, and we have used $T = \tilde{T} + T''$ and $\overline{\rho_f F_\alpha} = \overline{\rho}_f \tilde{F}_\alpha$.

Again, we shall drop the troublesome term (i.e., the second term in Eq. (C.8a)) without justification, but shall continue working either to justify its omission or to model it. Thus, our "final" form for the thermodynamic equation of state is

$$\overline{P} = \overline{\rho}\, R\, \tilde{T} \sum_{\alpha} \frac{\tilde{F}_\alpha}{M_\alpha} \qquad \text{(C.8b)}$$

Summarizing, Eqs. (C.1b)-(C.5b), (C.8b)-(C.10b), (C.14b) and (C.11a)-(C.13a) constitute (in 3D) a set of N+14 equations for the N values of F_α and $\overline{\rho}_f$, $\overline{\rho}_p$, the three $\tilde{v}_i$'s, the three $\tilde{u}_i$'s, $\overline{P}$, $\tilde{e}_f$, $\tilde{e}_p$, $\tilde{T}$, $\overline{\rho}$, and $\overline{\phi}$ plus the turbulent stress and diffusion terms and the chemical reaction and radiation terms. In the next report, we shall present our thinking on the turbulence closure problem (i.e., the modeling of the turbulent stress and diffusion terms), but we shall continue to ignore the chemical reaction and radiation terms.

We believe that the model developed in this section, even with the several terms that have been arbitrarily omitted, represents a significant improvement over other models that have been suggested insofar as fewer terms of possible

significance have been omitted than in any other second-order closure scheme.

APPENDIX D

THE EVOLUTION OF PARTICLE DISTRIBUTIONS FOR TURBULENT ENTRAINED FLOWS

INTRODUCTION

The number of particles at a given point in space at a given time can be subdivided into the numbers with particular sizes, velocities and temperatures. This distribution of particle numbers plays an important role in the behavior of turbulent flows involving particles. Thus the complete determination of the interaction of gas and particles involves simultaneous treatment of the conservation equations for the gas and particle flows and of an equation yielding the distribution of the number of particles with specific properties, e.g., size, velocities and temperature. At the present time, there exist no analyses involving such a complete treatment.

Our initial approach to the study of particle distributions is based on the assumption that the total number of particles is sufficiently small so that the characteristics of the gas flow are unaffected and therefore known. This corresponds to considering the particles to be carried along by, and consumed in, a turbulent, chemically-active, carrier gas. The information required to characterize the carrier gas depends on the analysis being employed for the determination of the distribution of particles. This approach, based on negligible influence of the particles on the gas, is considered a first step which will lead, in due course, to an appropriate treatment of the full, interacting case of practical interest.

Even with the crucial, simplifying assumption leading to consideration of particles in a known carrier gas, there appears to be no directly related literature applicable to turbulent flows of reacting solids. There are, however, several

contributions in related areas which can be brought to bear on this problem. For example, there is an extensive literature on the behavior of sprays and solid particles in inviscid flows, e.g., in nozzles. The review articles by Williams, 1962 and Marble, 1970 and the significant contribution of Shapiro and Erickson, 1957 provide entries into this literature. Also of interest to us is the literature concerned with the numerical simulation of the trajectories of particles of fixed size in turbulent flows since it suggests one approach to the study of our more complicated case of reacting flows. Peskin, 1974 should be consulted in this regard. Finally, the study of Lane, 1967 which is based on the theory of stochastic operators by Keller, 1964 and which is concerned with the behavior of electrons in a turbulent background gas may provide a convenient approach to the determination of the particle size distribution for weak turbulence.

A rather complete discussion of the equation for the particle size distribution and its solution are given below. Suppose we wish to determine the number of particles in appropriate infinitesimal "boxes" around the space point $\underset{\sim}{x}$ at time t with radius r, velocity $\underset{\sim}{u}$, and with temperature T^s, i.e., we desire $n(\underset{\sim}{x},t,r,\underset{\sim}{u},T^s)$. These quantities are considered to characterize sufficiently the properties of the particles; thus all particles are assumed to be essentially spherical and to have a uniform internal temperature. If this number as a function of the indicated variables is known, we can determine a variety of other properties of the particles by appropriate integration. For example, the time averaged particle cloud density at a point $\underset{\sim}{x}$ would be

$$\bar{\rho}_p = \lim_{\tau\to\infty} \tau^{-1} \rho^s 4\pi \int_0^\tau dt \int_0^\infty dr\, r^2 \int_{-\infty}^{\infty} d\underset{\sim}{u} \int_0^\infty dT^s n(\underset{\sim}{x},t,r,\underset{\sim}{u},T^s)$$

where ρ^s is the specific density of the solid. Other quantities depending only on the particles and their properties can be readily calculated.

The utilization of the number, n, of particles in the determination of the full interaction of the gas and particles involves additional considerations. To illustrate, consider the time averaged drag in the x_1-coordinate direction. Under the assumption of a Stokes drag law, the full and exact calculation is given by

$$\bar{f}_1(\underset{\sim}{x}) = \lim_{\tau\to\infty} \tau^{-1} \int_0^\tau dt \int_0^\infty dr\ r \int_{-\infty}^\infty du_2 \int_{-\infty}^\infty du_3 \int_0^\infty dT^s \int_{-\infty}^\infty dv_2 \int_{-\infty}^\infty dv_3$$
$$\int_{-\infty}^\infty du_1 \int_{-\infty}^\infty dv_1\ \mu(u_1-v_1)\ n(\underset{\sim}{x},t,r,\underset{\sim}{u},T^s,T,\underset{\sim}{v})$$

where $\underset{\sim}{v}$ is the gas velocity and μ is the coefficient of viscosity of the gas. Now the function $n(\underset{\sim}{x},t,r,\underset{\sim}{u},T^s,T,\underset{\sim}{v})$ implicitly involves integrations with respect to $\underset{\sim}{v}$ and T and thus an exact evaluation of $\bar{f}_1(\underset{\sim}{x})$ and other interaction terms requires additional approximations for solution in the case of full interaction between gas and particles.

In the equation for $n(\underset{\sim}{x},t,r,\underset{\sim}{u},T^s)$, the state of the carrier gas enters into the coefficients of that equation. The exact solution can be carried out to any desired space and time resolution by the method of characteristics coupled with time-dependent solutions of the hydrodynamic equations. This approach represents an extension of the numerical simulation techniques described by Peskin, 1974. However, for present purposes, approximate solutions are examined and, in particular, an approach based on correlations and leading to the determination of the time averaged particle number $\bar{n}(\underset{\sim}{x},r,\underset{\sim}{u},T^s)$, is given.

The incorporation of this approach into the hydrodynamic calculations with an approximate treatment of the interaction appears promising.

It is perhaps appropriate to note that these studies of the behavior of particles in a turbulent carrier gas will prove useful in the development of appropriate phenomenology for the source terms describing the chemical interaction effect. Information concerning the chemical reactions between a particle of specified temperature, T^s, and a surrounding quiescent gas of specified temperature and composition must be incorporated into the description of time-averaged source terms which account for the fluctuations of gas properties and for the distribution of particle sizes and temperatures. This problem is analogous to, but probably more difficult than, the corresponding description of the mean creation terms in turbulent reacting flows devoid of particles; the interaction of turbulence and chemical reaction in gas flows free of particles is a largely unsolved problem which is the subject of current active research [Libby and Williams, 1976]. We anticipate that our study of particle size distributions will, at the least, provide information about the sensitivity of the source terms to the various contributing components of the gas flow turbulence and may suggest an effective phenomenology to be incorporated into the hydrodynamic calculations so that the essential effects of turbulence are accounted for.

CONSERVATION EQUATION FOR $n(\underset{\sim}{x},t,r,\underset{\sim}{u},T^s)$

We consider the function $n(\underset{\sim}{x},t,r,\underset{\sim}{u},T^s)$ which gives the number of particles in the nine-dimensional, infinitesimal volume surrounding the point identified with the indicated variables.*

*Note that the dimensions of n are, e.g., $cm^{-3}\ sec^{-1}\ cm^{-1}\ (cm/sec)^{-3}\ (°K)^{-1} = cm^{-7}\ sec^{2}(°K)^{-1}$.

Physical arguments suggest a ready extension of the conservation equation for the particle number provided by Shapiro and Erickson [1957] and Williams [1962]. We have

$$\partial n/\partial t + u_k(\partial n/\partial x_k) + \partial(Rn)/\partial r + \partial(F_k n)/\partial u_k + \partial(Hn)/\partial T^s = 0 \qquad (D.1)$$

where

$R = dr/dt$, the rate of change or particle size;

$F_k = du_k/dt$, the rate of change of the kth velocity component of a particle; and

$H = dT^s/dt$, the rate of change of particle temperature.

If appropriate functional forms for the coefficients, R, F_k and H, are specified, Equation (D.1) is a linear, first-order, hyperbolic equation whose exact solution to any desired space and time resolution can, in principle, be obtained by application of the method of characteristics. Although such exact solutions are probably not appropriate for our studies, their consideration is instructive and therefore worth discussing.

To proceed, it is unnecessary to be explicit about the coefficients in Equation (D.1); rather it is sufficient to indicate that they are given, explicit functions of the independent variables, u_k, r, and T^s and depend implicitly on the other independent variables, x_k and t, through their explicit dependence on the gas properties, ρ, v_k, T, $Y_1,....Y_N$ where ρ is the gas density; v_k the kth component of the gas velocity; T is the gas temperature; and the Y_i's are the mass fractions of the gas. All of these quantities are treated as known functions of the space coordinates x_k and time, t. If we were

actually carrying through the calculations under discussion, these functions could be generated by a hydrodynamic program for a turbulent gas flow without particles present so that at each space-time point the R, F_k, and H coefficients would be explicit functions of only the independent variables u_k, r, and T^s. Such an approach would represent an extension to a more complex situation of the numerical simulations described by Peskin, 1974.

. The exact solution of Equation (D.1) by the method of characteristics is given by a solution of a system of ordinary differential equations, namely

$$dn/dt = -n(\partial R/\partial r + \partial F_k/\partial u_k + \partial H/\partial T^s) \tag{D.2}$$

$$dx_k/dt = u_k \tag{D.3}$$

$$dr/dt = R \tag{D.4}$$

$$du_k/dt = F_k \tag{D.5}$$

$$dT^s/dt = H \tag{D.6}$$

These equations are to be solved subject to suitable initial conditions; for purposes of exposition, we postpone detailed discussion of such conditions for the present.

The physical implication of Equations (D.2,...6) is as follows: The last four equations give the trajectory through the eight-dimensional space identified with the coordinates x_k, r, u_k, and T^s of particles whose number and position in that eight-dimensional space at time zero are given by the initial conditions. The first equation describes the history of the population along that trajectory; for the situations of interest to us, wherein the particles are being consumed, the history is of interest until the original population is entirely obliterated, i.e., until $n = 0$.

Exact solutions to Equations (D.2,...6) can be used to develop, by numerical experimentation, the statistics of the number distribution, n. The point of view in this regard is as follows: Imagine that two turbulent gas flows with different velocities and state properties mix in some fashion and that their space-time behavior is known. Along a streamwise line indicative of the origin of mixing, introduce an initial number of particles of known size and temperature, but with a spectrum of particle velocities, in one stream and calculate their trajectories and histories to extinction by solving Equations (D.2,...6). If this calculation is repeated many times with the same initial conditions except for a spectrum of initial velocities, it is possible to develop a sufficiently large number of realizations so that the statistics of that population of particles with that size and temperature passing that particular spatial point can be developed to calculate $n(\underset{\sim}{x},t,r,\underset{\sim}{u},T^s)$. These calculations must be repeated at different initial spatial points and with different initial r and T^s. Clearly, a considerable calculation is required. Accordingly, approximate solutions are indicated.

THE COEFFICIENTS OF THE CONSERVATION EQUATION

Before discussing approximate solutions to Equation (D.1), it is worthwhile to discuss possible forms for the coefficients appearing therein. In developing these coefficients, Soo, 1967 and Williams, 1962 are useful references. The easiest of the three coefficients is F_k. If we assume the main contribution to the force on a particle is that associated with Stokes drag, then the dynamics of a single particle result in

$$F_k = -9\mu(u_k - v_k)/\rho^s r^2 \qquad (D.7)$$

The treatment of the other two coefficients is conveniently considered in terms of two phases of particle behavior. If we assume the particles are initially cold and therefore chemically inert, there will be a heating up phase in their history during which no change in size occurs so that $R = 0$. During this phase, the heat conduction between the particle and the gas can be represented as*

$$H = 3\mu\, c^s(T - T^s)/r^2\, \rho^s\, c^s \qquad (D.8)$$

where c_p^s is the coefficient of specific heat of the solid.

During the second phase of particle behavior, a reasonable, simplifying approximation might be that the particle remains at a fixed temperature T_c while chemical reaction leading to reduction in particle size occurs. The temperature, T_c, effectively defines the end of the first phase and the beginning of the second. According to this approximation, $H = 0$ and we need only represent R. The description of the rate of loss of particle mass which can be directly employed to determine R is complicated because the phenomenology of both chemical and fluid mechanical effects are involved. Thus, at the present time, we can only suggest the type of representation likely to be developed.

If we assume the particle to be carbon and to be subject to direct hetereogeneous attack by oxygen molecules, the reaction mechanism can be taken to be

$$\frac{1}{2}\, O_2 + \text{surface} \rightarrow O + C \rightarrow CO \qquad (D.9)$$

Furthermore, if we make several simplifying assumptions

*See Equation (2.126) of Soo [1967], neglect radiation and assume the Prandtl number of the gas is roughly unity.

concerning the aerothermochemistry and transport properties of the gas mixture surrounding the particle, we find (c.f. Appendix A)

$$R = \frac{1}{\rho^s} \left\{ \frac{P_{0_2}}{\frac{1}{K_1} + \frac{1}{K_0}} \right\} \qquad (D.10)$$

APPROXIMATE ANALYSIS BASED ON CORRELATIONS

One method of obtaining approximate solutions to Equation (D.1), at least for the time-averaged number densities, is based on averaging and correlations. To discuss this method we shall explicitly invoke the model of particle behavior based on the two distinct phases and shall consider only the initial phase during which the particle size does not change, but rather the particle temperature increases to T_c. The extension to include description of the second phase is straightforward.

For the first phase of particle history, the time average of Equation (D.1) gives

$$u_k(\partial\bar{n}/\partial x_k) + \partial(\bar{F}_k\,\bar{n} + \overline{F_k'n'})/\partial u_k + \partial(\bar{H}\,\bar{n} + \overline{H'n'})/\partial T^s = 0 \qquad (D.11)$$

where the bar denotes time-averaged and the prime the fluctuation. The effect of turbulence in the carrier gas on the mean number density of particles in the seven-dimensional space of $\underset{\sim}{x}$, $\underset{\sim}{u}$ and T_p is contained in the correlations $\overline{F_k'n'}$ and $\overline{H'n'}$.

Explicit expressions for F_k' and H' in terms of the fluctuations of the gas properties can be readily obtained from Equations (D.7,8). For present purposes, it is sufficient to work directly in terms of F_k' and H', but we do reflect the functional forms for F_k and H in the development below.

Equation (D.11) cannot be used to calculate n unless expressions for $\overline{F_k'n'}$ and $\overline{H'n'}$ are provided in some fashion. There are several alternative approaches to these expressions. In analogy with the classical treatment of turbulence, we can introduce a gradient approximation so that, e.g., $\overline{F_k'n'} \propto F'^2\, \partial\bar{n}/\partial u_k$ where the constant of proportionality is chosen in some fashion. A second approach corresponds to second-order closure; the starting point in this approach is an equation for the fluctuations in number density. Subtraction of Equations (D.1) and (D.11) yields

$$\partial n'/\partial t + u_k(\partial n'/\partial x_k) + \partial(\bar{F}_k n' + F_k'\bar{n} + F_k'n' - \overline{F_k'n'})/\partial u_k$$

$$+ \partial(\bar{H}\, n' + H'\bar{n} + H'n' - \overline{H'n'})/\partial T^s = 0 \qquad \text{(D.12)}$$

If this equation is multiplied by F_k' and averaged and then by H' and averaged, we find the two equations

$$u_k \partial(\overline{F_k'n'})/\partial x_k + \partial(\bar{F}_k\, \overline{F_k'n'} + \tfrac{1}{2}\, \overline{F_k'^2 n'})/\partial u_k + \partial(\bar{H}\, \overline{F_k'n'} + \overline{F_k'H'n'}) =$$

$$- \tfrac{1}{2}\, \partial(\bar{n}\, \overline{F_k'^2})/\partial u_{kp} - \partial(\bar{n}\, \overline{F_k'H'})/\partial T^s + \lim_{\tau \to 0} \partial\, \overline{(n'(\underset{\sim}{x},t,r,\underset{\sim}{u},T^s)\cdot}$$

$$\overline{F_k'(\underset{\sim}{x} + \underset{\sim}{u}\tau, t + \tau, r, \underset{\sim}{u} + \underset{\sim}{\bar{F}}\tau)}/\partial\tau \qquad \text{(D.13)}$$

$$u_k \; \partial(\overline{H'n'})/\partial x_k + \partial(\overline{F}_k\overline{H'n'} + \overline{F_k'H'n'})/\partial u_k + \partial(\overline{H}\;\overline{H'n'} + \tfrac{1}{2}\overline{H'^2n'})/\partial T^s$$

$$= -\partial(\overline{F_k'H'n})/\partial u_k - \tfrac{1}{2}\partial(\overline{H'^2}\overline{n})/\partial T^s + \lim_{\tau\to 0} \partial(\overline{n'(\underset{\sim}{x},t,r,\underset{\sim}{u},T^s)\cdot H'(\underset{\sim}{x} + \underset{\sim}{u}\tau, t+\tau, r, \underset{\sim}{u} + \underset{\sim}{\overline{F}}\tau, T + \overline{H}\tau)})/\partial\tau \qquad (D.14)$$

These equations can be interpreted as conservation equations for the desired correlations, $\overline{F_k'n'}$ and $\overline{H'n'}$. However, these new equations are not complete or "closed" either, in this case because of the higher-order correlations, $\overline{F_k'H'n'}$, $\overline{H'^2n'}$, $\overline{F_k'^2n'}$, and because of the last terms on the right side of each equation. These latter terms, which must be modeled in some fashion, represent the correlation between the fluctuations in number density and, e.g., in F_k' along the mean trajectory of the particles in the nine-dimensional space.

Additional equations for the higher-order correlations can be developed in the same fashion as used for Equations (D.13) and (D.14), but as is typical of the closure problem, new higher-order correlations and additional terms such as the last terms on the right sides will arise and require special treatment. All of these symptoms can be related to those usually encountered in the phenomenology of turbulent flows.

Additional study of this approach is indicated before numerical analysis is appropriate. It is worth noting that all of the equations, e.g., those for $\overline{n}$, $\overline{F_k'n'}$ and $\overline{H'n'}$, are hyperbolic; the solutions are as indicated by Equations (D.2,...6) but with the trajectories corresponding to the mean values of F_k and H, i.e., to $\overline{F}_k$ and $\overline{H}$. It should also be noted that the effects of the turbulence of the carrier gas are explicitly taken into account; in particular, when this analysis is carried out for the second phase of the history of the particles, i.e., when chemical reaction and reduction of particle size occurs, the influence of R and R' will enter.

There are perhaps other means for extracting useful information concerning the evolution of particle distributions from Equation (D.1). For example, the method of stochastic operators [Lane, 1967 and Keller, 1964] may be applicable at least for the case of weak turbulence. In assessing other approaches, we recognize the desirability, if not the necessity, of having a means of analysis which can be incorporated with some further rational approximation into the computation of the coupled equations for the conservation of gas and particles.

APPENDIX E

FINITE ELEMENT-FINITE DIFFERENCE SOLUTION OF THE EQUATIONS OF COMPRESSIBLE VISCOUS FLOW

The equations to be treated here are the Navier-Stokes equations for compressible viscous flow; for simplicity, thermal effects are not included, but it is very straightforward to do so. The continuity equation is

$$\frac{\partial}{\partial t}\rho + \sum_{j=1}^{Nd} \frac{\partial}{\partial x_j}(\rho v_j) = 0 \qquad \text{(E.1)}$$

where ρ is fluid density, t is time, x_j are the space coordinates, v_i the fluid velocity components and Nd the number of dimensions. The momentum equations are

$$\frac{\partial}{\partial t}(\rho v_i) + \sum_{j=1}^{Nd} \frac{\partial}{\partial x_j}(\rho v_i v_j) - \mu \sum_{j=1}^{Nd} \left(\frac{\partial}{\partial xj} \frac{\partial}{\partial x_i} v_j + \frac{\partial}{\partial x_j} v_i \right)$$

$$+ \frac{\partial}{\partial x_i} p = 0 \qquad \text{(E.2)}$$

where μ is the fluid viscosity and p the pressure.

The procedure to be used for the solution of Eqs. (E.1) and (E.2) is a finite element-finite difference method [see, e.g., Zienkiewicz, 1971 for a discussion of the finite element], where the finite theory difference character is related to the application of the basic philosophy of the so-called ICE technique [Harlow, et al., 1974] (Implicit Continuous Eulerian). This finite difference technique has proved successful in treating low-speed compressible flow problems.

The finite element approach to continuum field problems assumes the continuum to be divided into elements, with nodes located either on the boundaries or in the interior of the elements (see Figure 1). We will assume the nodes are on element boundaries. Furthermore, to incorporate the ICE philosophy, density and pressure will be assumed to be centered at the elements, and velocity at the nodes. We will use three types of interpolation functions for expanding the dependent variables; these are shown in Figure 2.

In the following, right superscripts refer to elements (capital letters) or nodes (lower case), right subscripts to Cartesian components, and left superscripts to time levels. The weighted residual technique [Zienkiewicz, 1971] will be applied here.

The dependent variables are expanded in terms of the interpolation functions:

$$\rho = \sum_{L=1}^{Ne} \rho^L \, M^L \tag{E.3}$$

$$p = \sum_{L=1}^{Ne} p^L \, M^L \tag{E.4}$$

$$\rho v_i = \sum_{m=1}^{Nn} (\rho v_i)^m \, M^m \tag{E.5}$$

$$\overline{\rho v_i v_j} = \sum_{m=1}^{Nn} (\rho v_i v_j)^m \, N^m \tag{E.5}$$

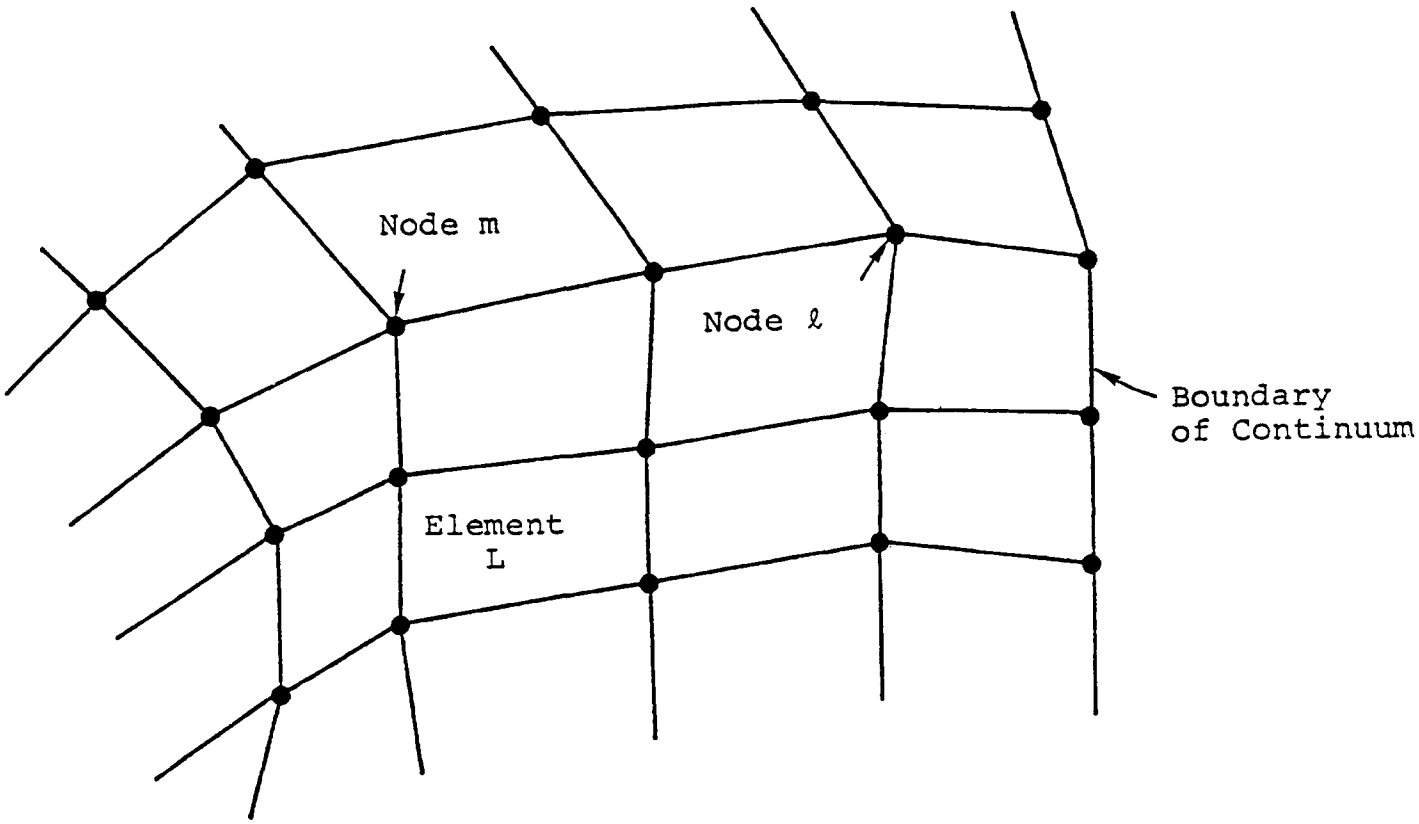

Figure 1. Discretization of a continuum into elements with nodes at element corners. The node and element nomenclature is apropos to the description of interpolation functions in Figure 2.

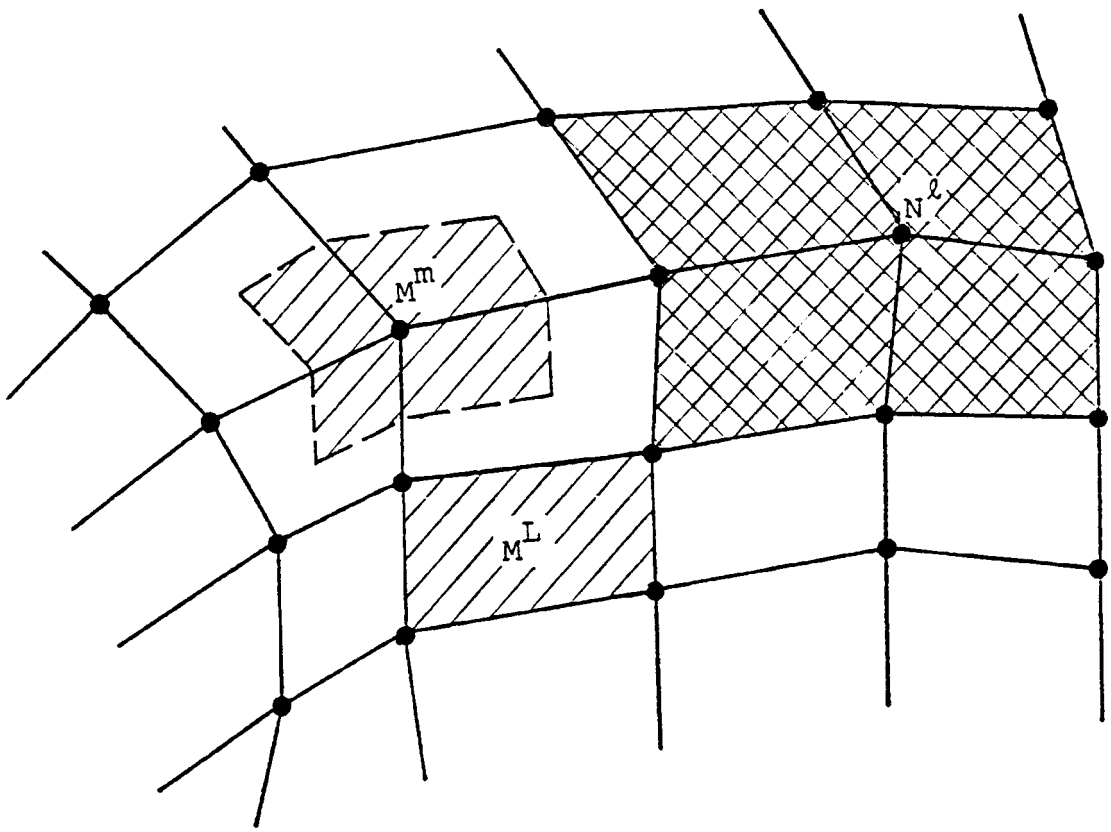

Figure 2. Showing regions in which interpolation functions M^m, N^ℓ and M^L are nonzero. The functions M^m and M^L are equal to unity in the single-shaded regions, zero elsewhere; N^ℓ is equal to unity at node ℓ, and is zero outside and on the boundary of the double-shaded region, inside which it is continuous.

$$\overline{\rho v_i} = \sum_{m=1}^{Nn} (\rho v_i)^m \, N^m \qquad \text{(E.7)}$$

$$\overline{v_i} = \sum_{m=1}^{Nn} v_i^m \, N^m \qquad \text{(E.8)}$$

where ρ^L, $(\rho v_i)^m$, etc. are the discrete values of those variables associated with element L or node m. Here, Ne is the number of elements and Nn the number of nodes.

A finite difference equation is used for the continuity equation:

$$\frac{1}{\Delta t_n} V_L \, {}^{n+1}\delta\rho^L + \int_{S_L} \sum_{j=1}^{Nd} {}^{n+1}(\overline{\rho v_j}) \, dS_j = 0 \qquad \text{(E.9)}$$

where S_L is the boundary of element L, V_L is the volume of element L, and dS_j is the differential outward normal area on S_L. Here

$$ {}^{n+1}\delta\rho^L \equiv {}^{n+1}\rho^L - {}^{n}\rho^L \qquad \text{(E.10)}$$

Equation (E.9) results from applying Gauss' law to Eq. (E.1), and assuming the density is constant throughout element L at each time step. Using the expansion of Eq. (E.7), Eq. (E.9) leads to

$$ {}^{n+1}\delta\rho^L = \Delta t_n \sum_{m=1}^{Nn} \sum_{j=1}^{Nd} R_j^{Lm} \, {}^{n+1}(\rho v_j)^m \qquad \text{(E.11)}$$

where

$$R_j^{Lm} = -\int_{S_L} N^m \, dS_j \tag{E.12}$$

The momentum equation, Eq. (E.2), is treated by a more purely finite element approach:*

$$\int M^{\ell} \frac{1}{\Delta t_n} \left[{}^{n+1}(\rho v_i) - {}^{n}(\rho v_i) \right] dV$$

$$+ \int N^{\ell} \sum_{j=1}^{Nd} \frac{\partial}{\partial x_j} {}^{n}(\overline{\rho v_i v_j}) \, dV$$

$$- \int N^{\ell} \mu \sum_{j=1}^{Nd} \frac{\partial}{\partial x_j} \left(\frac{\partial}{\partial x_i} {}^{n}\bar{v}_j + \frac{\partial}{\partial x_j} {}^{n}\bar{v}_i \right) dV$$

$$+ \int N^{\ell} \frac{\partial}{\partial x_i} {}^{n+1}p \, dV = 0 \tag{E.13}$$

where

$${}^{n+1}p = {}^{n}p + {}^{n}\left(\frac{\partial p}{\partial \rho}\right) \left({}^{n+1}\rho - {}^{n}\rho \right) \tag{E.14}$$

Using the appropriate expansions in Eq. (E.13), and integrating by parts, we obtain

---

*In our recent version of the code we have introduced a finite difference approach to this equation also.

$$\frac{1}{\Delta t_n} V^{\ell}\left[{}^{n+1}(\rho v_i)^{\ell} - {}^{n}(\rho v_i)^{\ell}\right] = -\int N^{\ell} \sum_{j=1}^{Nd} {}^{n}(\overline{\rho v_i v_j})\, dS_j$$

$$+\int \sum_{j=1}^{Nd} \left(\frac{\partial}{\partial x_j} N^{\ell}\right) {}^{n}(\overline{\rho v_i v_j})\, dV$$

$$+\int N^{\ell}\, \mu \sum_{j=1}^{Nd} \left(\frac{\partial}{\partial x_i} {}^{n}\bar{v}_j + \frac{\partial}{\partial x_j} {}^{n}\bar{v}_i\right) dS_j$$

$$-\int \sum_{j=1}^{Nd} \left(\frac{\partial}{\partial x_j} N^{\ell}\right) \mu \left(\frac{\partial}{\partial x_i} {}^{n}\bar{v}_j + \frac{\partial}{\partial x_j} {}^{n}\bar{v}_i\right) dV$$

$$-\int N^{\ell}\, {}^{n}p\, dS_i + \int \left(\frac{\partial}{\partial x_i} N^{\ell}\right) {}^{n}p\, dV$$

$$+\int \left(\frac{\partial}{\partial x_i} N^{\ell}\right) \sum_{M=1}^{Ne} M^{m}\, {}^{n}\left(\frac{\partial p}{\partial \rho}\right)^{M} {}^{n+1}\delta\rho^{M}\, dV \qquad \text{(E.15)}$$

so that

$${}^{n+1}(\rho v_i)^{\ell} = {}^{n}p_i^{\ell} + \Delta t_n \sum_{M=1}^{Ne} {}^{n}\left(\frac{\partial p}{\partial \rho}\right)^{M} Q_i^{\ell M}\, {}^{n+1}\delta\rho^{M} \qquad \text{(E.16)}$$

where

$$
\begin{aligned}
{}^{n}p_i^{\ell} = {}^{n}(\rho v_i)^{\ell} + \Delta t_n \, V_{\ell}^{-1} \Bigg\{ & - \sum_{m=1}^{Nn} \sum_{j=1}^{Nd} \left(\int N^{\ell} N^{m} \, dS_j \right) {}^{n}(\rho v_i v_j)^{m} \\
& + \sum_{m=1}^{Nn} \sum_{j=1}^{Nd} \left[\int \left(\frac{\partial}{\partial x_j} N^{\ell} \right) N^{m} \, dV \right] {}^{n}(\rho v_i v_j)^{m} \\
& + \sum_{m=1}^{Nn} \sum_{j=1}^{Nd} \left[\int N^{\ell} \, \mu \left(\frac{\partial}{\partial x_j} N^{m} \right) dS_j \right] {}^{n}v_i^{m} \\
& + \sum_{m=1}^{Nn} \sum_{j=1}^{Nd} \left[\int N^{\ell} \, \mu \left(\frac{\partial}{\partial x_i} N^{m} \right) dS_j \right] {}^{n}v_j^{m} \\
& - \sum_{m=1}^{Nn} \sum_{j=1}^{Nd} \left[\int \left(\frac{\partial}{\partial x_j} N^{\ell} \right) \mu \left(\frac{\partial}{\partial x_j} N^{m} \right) dV \right] {}^{n}v_i^{m} \\
& - \sum_{m=1}^{Nn} \sum_{j=1}^{Nd} \left[\int \left(\frac{\partial}{\partial x_j} N^{\ell} \right) \mu \left(\frac{\partial}{\partial x_i} N^{m} \right) dV \right] {}^{n}v_j^{m} \\
& - \int_{S_u} N^{\ell} \, {}^{n+1}p \, dS_i - \int_{S_f} N^{\ell} \, {}^{n}p \, dS_i \\
& + \int \left(\frac{\partial}{\partial x_i} N^{\ell} \right) {}^{n}p \, dV \Bigg\}
\end{aligned}
\qquad \text{(E.17)}
$$

and

$$Q_i^{\ell M} = V_\ell^{-1} \left\{ -\int_{S_f} N^\ell \underset{\sim}{M}^M \, dS_i + \int \left(\frac{\partial}{\partial x_i} N^\ell \right) M^M \, dV \right\} \qquad \text{(E.18)}$$

where S_u is that part of the grid boundary on which the pressure is fixed, S_f the part where the pressure is unknown at time t_{n+1}.

The solution of the equations at time t_{n+1} is accomplished by substituting Eq. (E.16) into Eq. (E.11) and simply solving for the ${}^{n+1}\delta\rho^L$. The linear system to be solved is

$$\sum_{M=1}^{Ne} {}^{n}K^{LM} \, {}^{n+1}\delta\rho^M = \Delta t_n \left[\sum_{(m,j)\in D_u} R_j^{Lm} \, {}^{n+1}(\rho v)_j^m + \sum_{(m,j)\in D_f} R_j^{Lm} \, {}^{n}p_j^m \right] \qquad \text{(E.19)}$$

where D_u is the set of degrees of freedom at which $(\rho v)_j^m$ are fixed at time t_{n+1}, and D_f the set at which the ρv are unknown. In Eq. (E.19),

$${}^{n}K^{LM} = \delta_{LM} - \Delta t_n^2 \, {}^{n}\left(\frac{\partial p}{\partial \rho} \right)^M T^{LM} \qquad \text{(E.20)}$$

where

$$T^{LM} = \sum_{(m,j)\in D_f} R_j^{Lm} \, Q_j^{mM} \qquad \text{(E.21)}$$

and $\delta_{LM} = 1$ if $L = M$

$= 0$ if $L \neq M$ (E.22)

An earlier version of the above procedure has been developed; it is a finite element scheme, fully implicit in pressure (or density) and velocity, which treats viscous, unsteady compressible flow in two or three dimensions. Several sample calculations have been performed with this code.

Figure 3 shows the computational grid used for the calculation of steady, incompressible viscous flow in a two-dimensional meandering channel. Boundary conditions and problem parameters are shown on the figure. Figure 4 shows the velocity vectors at the grid nodes in the steady state.

Two calculations were performed of steady compressible Poiseuille-like viscous flow in a plane two-dimensional channel. The computational grids and boundary conditions are shown in Figures 5 through 7. In each case the pressure (or, equivalently, the density) is specified at the inlet and outlet of the channel. Only half the width of the channel is included in the grid, because of the symmetry of the problems. For the problem of Figure 5, the flow is almost compressible, i.e., the density difference between the inlet and outlet is small; the numerical solution to the problem (the velocity vectors are shown in Figure 6) is almost identical to the theoretical solution of incompressible plane Poiseuille flow for density $\rho = 1$.

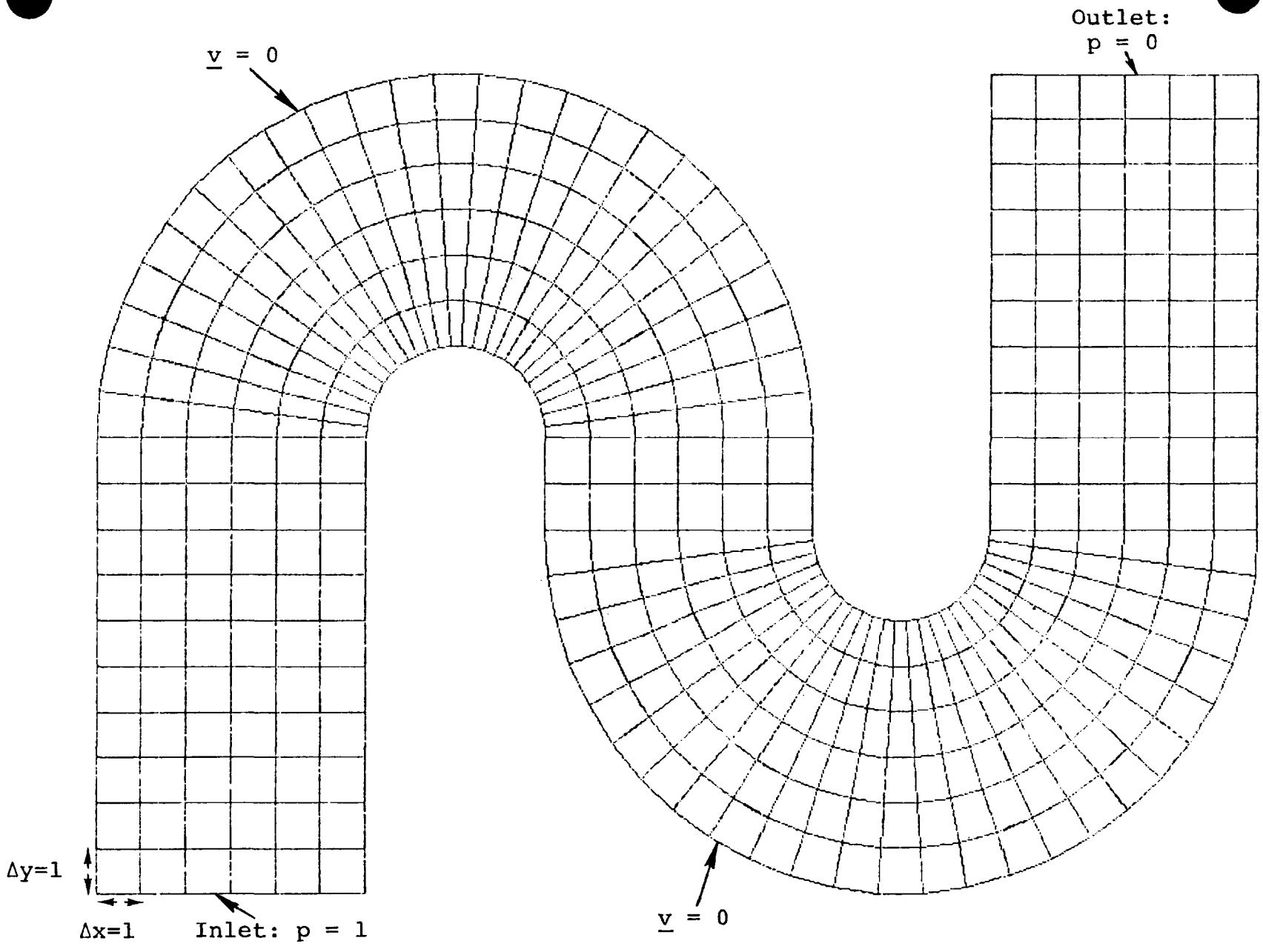

Figure 3. Incompressible viscous steady channel flow. $p = \mu = 1$.

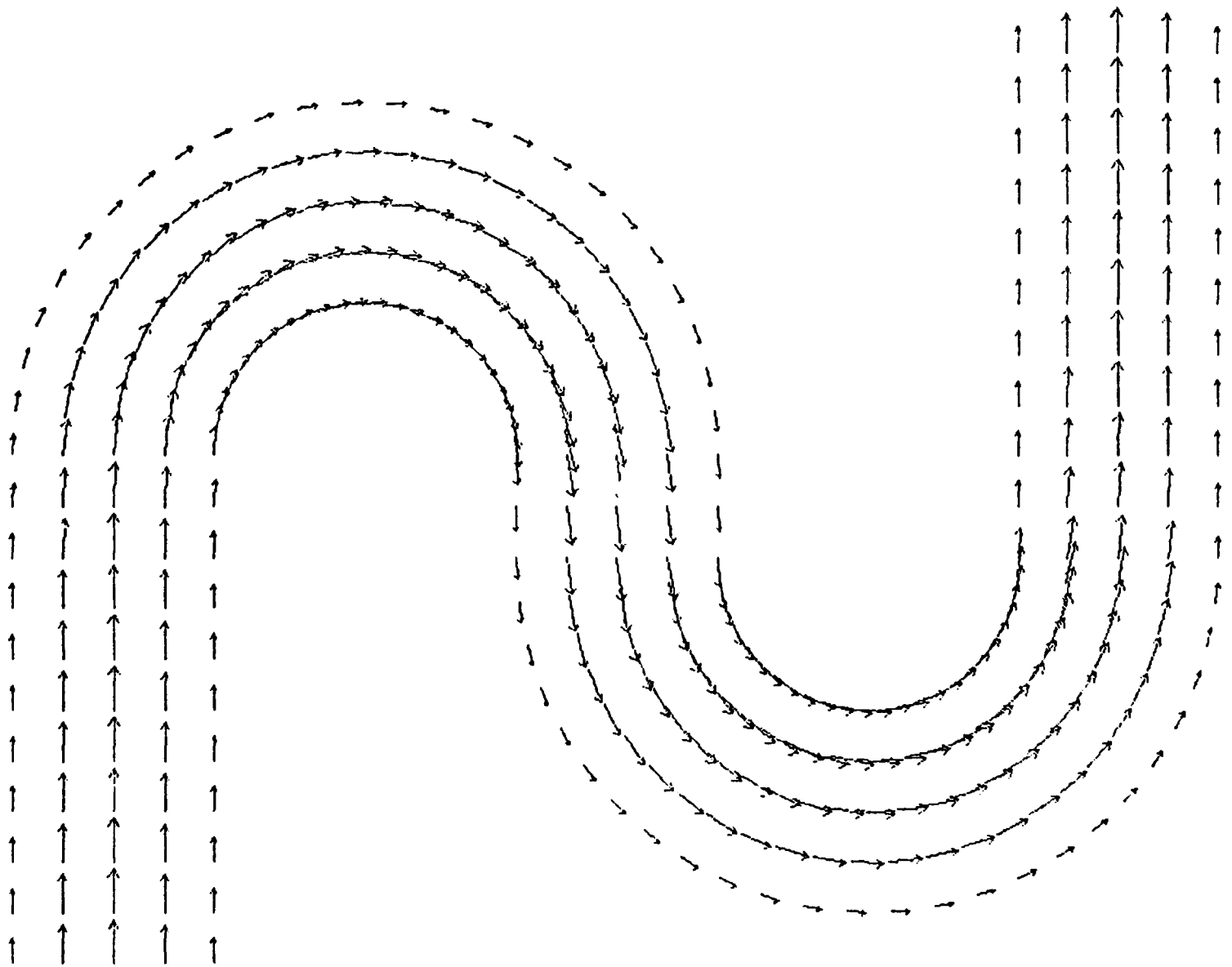

Figure 4. Velocity vectors in steady flow for problem of Figure 3. The maximum velocity is 0.0818 in magnitude.

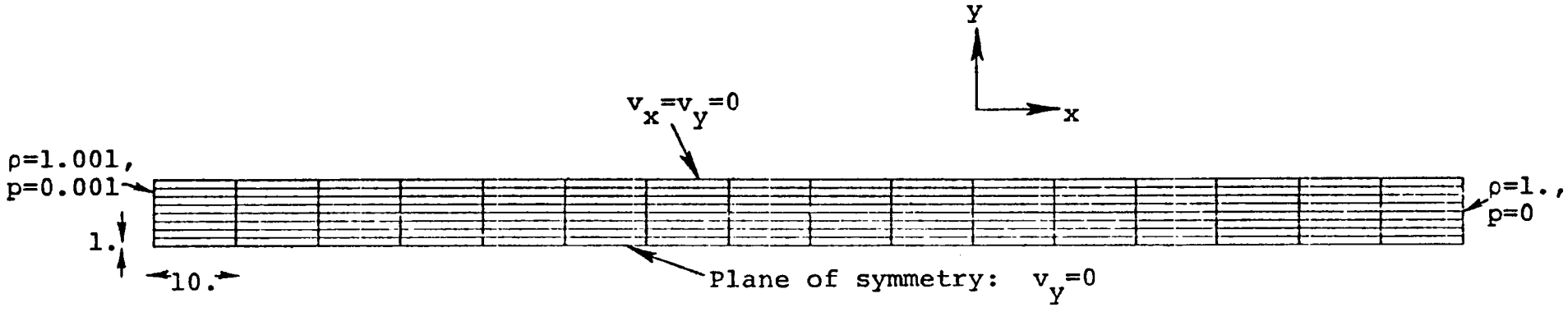

Figure 5. Almost compressible steady Poiseuille-like flow: $p = A\ (\rho/\rho_0-1)$, $A = \rho_0 = \mu = 1$.

Figure 6. Velocity vectors in steady flow for problem of Figure 5. The maximum velocity is 2.00×10^{-4} in magnitude.

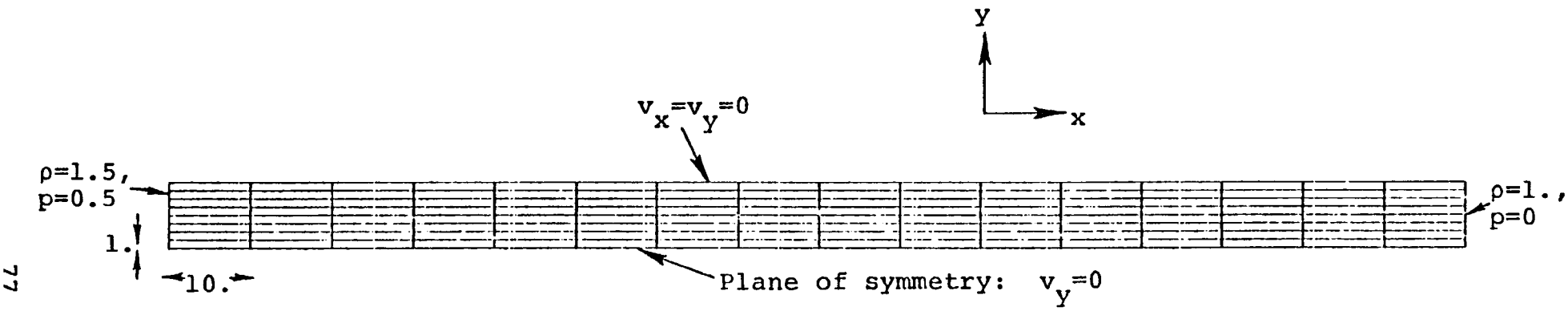

Figure 7. Compressible steady Poiseuille-like flow: $p = A\,(\rho/\rho_0 - 1)$, $A = \rho_0 = \mu = 1$.

The problem of Figure 7 is similar to that of Figure 5 except that the flow is highly compressible, with a much larger density difference between inlet and outlet. Velocity vectors for this problem are shown in Figure 8. Here it is seen that the flow is accelerating down the channel, as expected.

A calculation of the evolution in time of Couette flow between two plates has been performed using the unsteady flow option of the code. The problem grid and initial and boundary conditions are shown in Figure 9. Velocity vectors at selected computational cycles are shown in Figures 10-13. Due to the symmetry of the problem it was necessary to use only one element length parallel to the plates. Figure 14 shows a comparison between the numerical and exact [Schlichting, 1960] solutions to the problem.

Figure 8. Velocity reactors in steady flow for problem of Figure 7. The maximum velocity is 0.124 in magnitude.

$p = p_0 \rho/\rho_0$

$p_0 = \rho_0 = \mu = 1$

Initial conditions:

$\rho = \rho_0$,

$v_x = v_y = 0$

everywhere

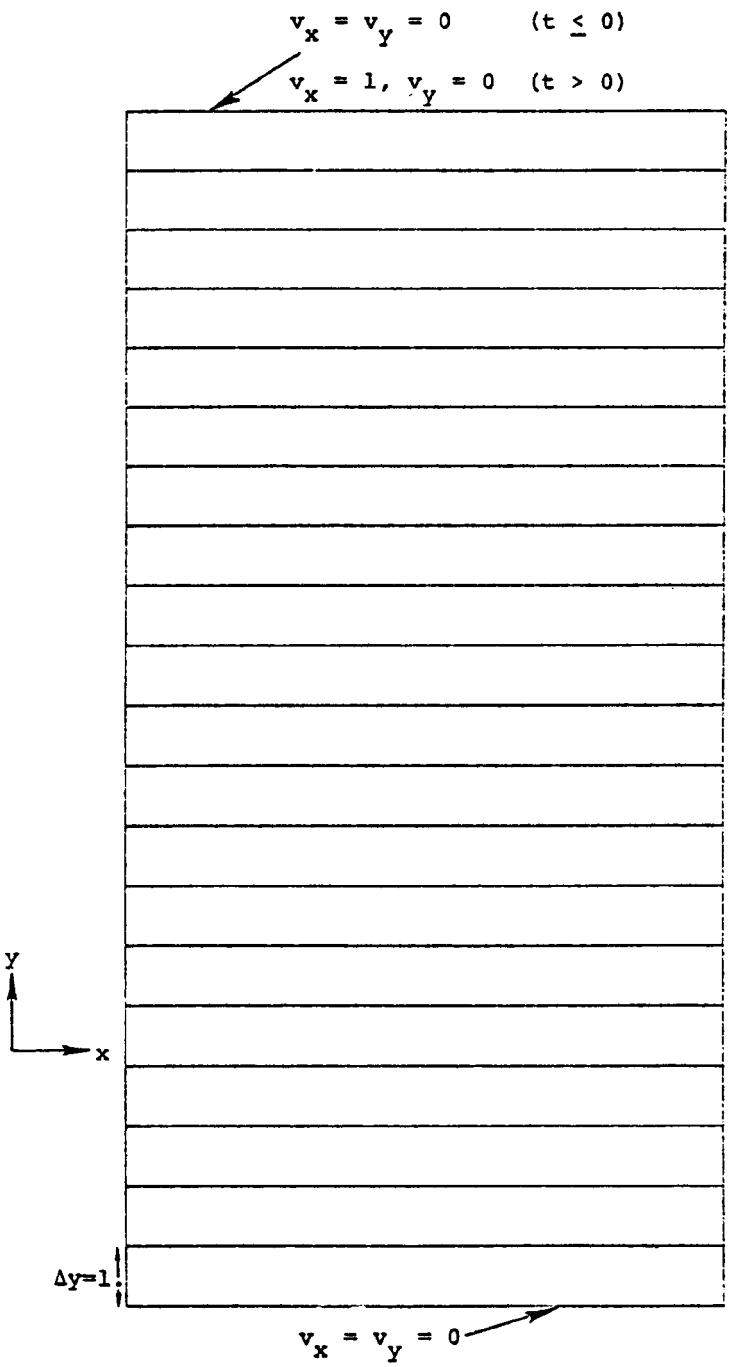

Figure 9. Computational grid, initial and boundary conditions for Couette flow development problem.

Figure 10. Velocity vectors in Couette flow formation, cycle 29, t = 1.49.

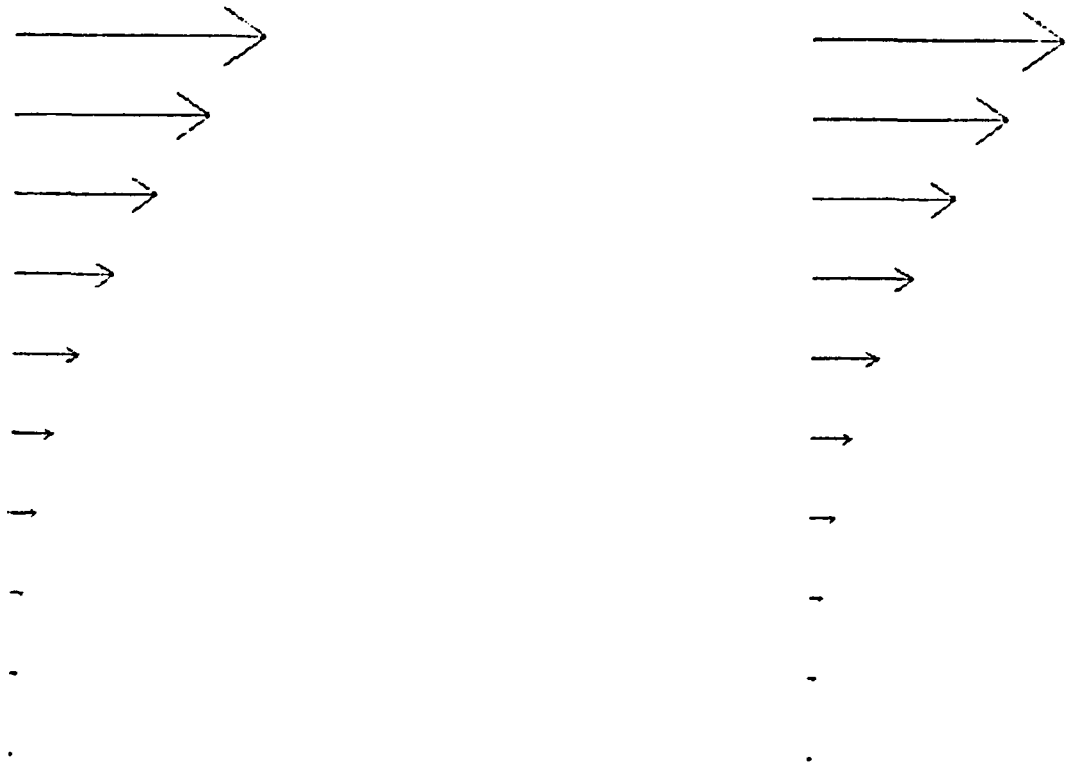

Figure 11. Velocity vectors in Couette flow formation, cycle 44, t = 6.53.

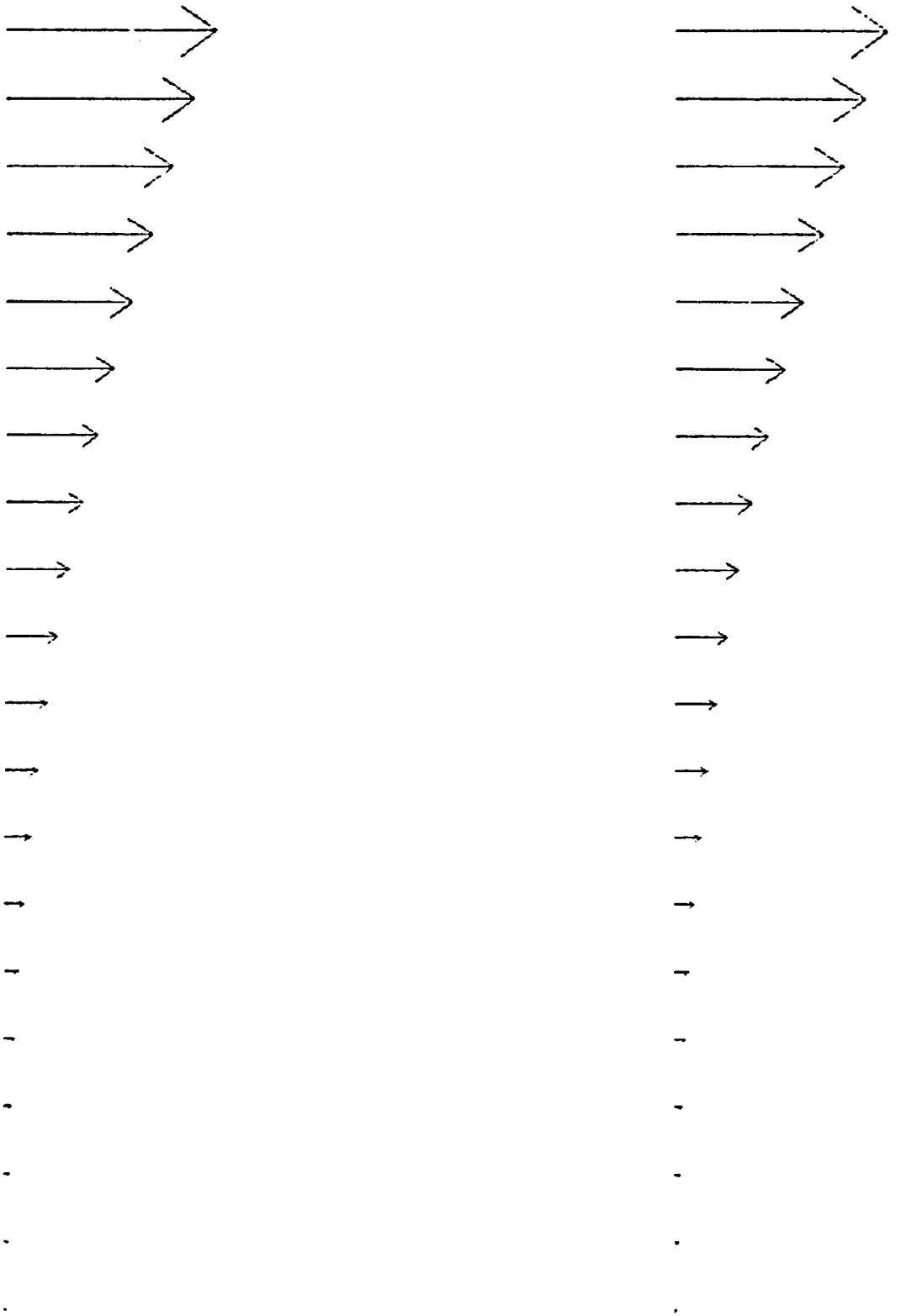

Figure 12. Velocity vectors in Couette flow formation, cycle 60, t = 30.35.

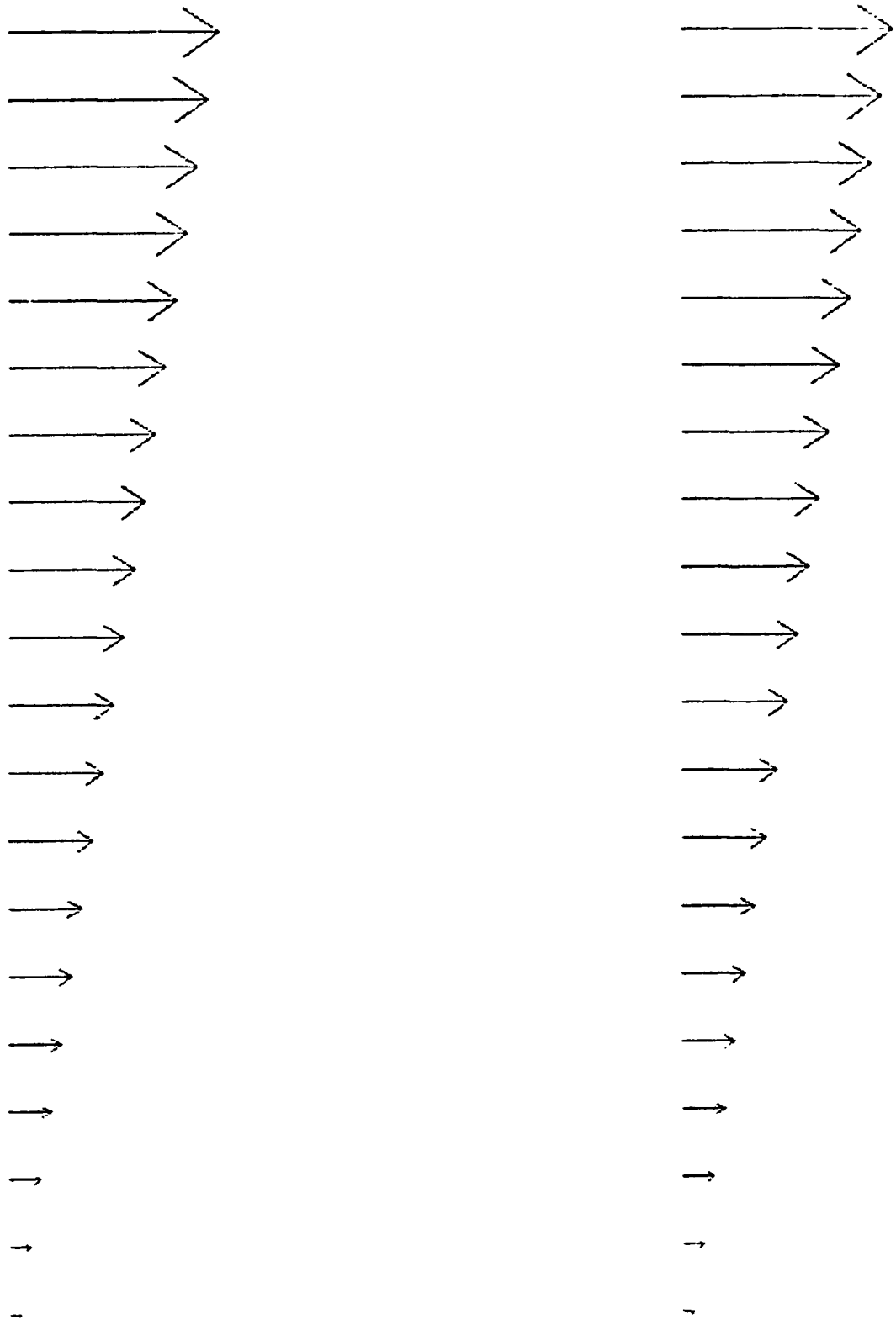

Figure 13. Velocity vectors in Couette flow formation, cycle 90, t = 531.20.

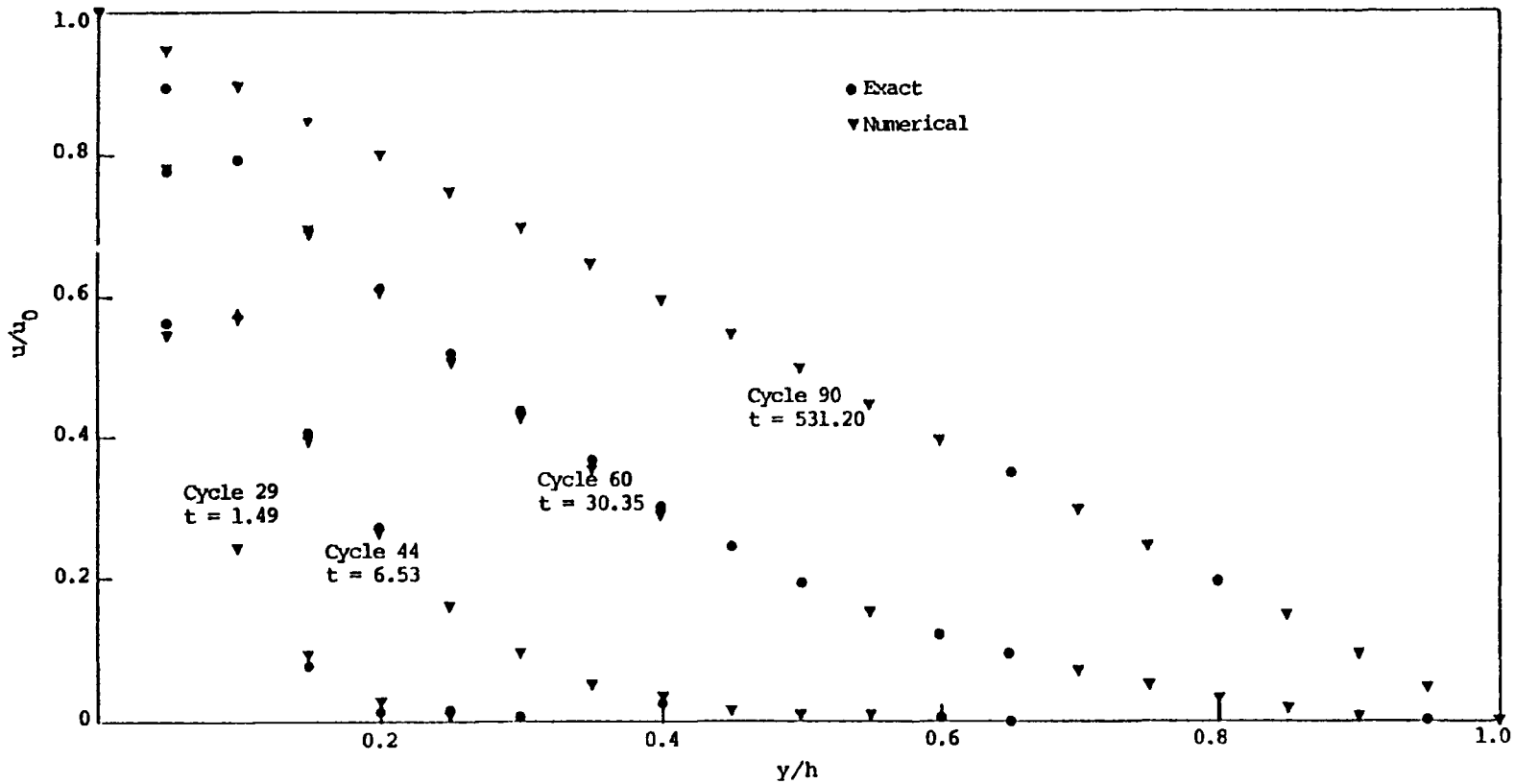

Figure 14. Comparison of exact and numerical solutions in Couette flow development problem.

REFERENCES

Anderson, T. B. and R. Jackson [1967], Ind. and Eng. Chem. Fund., 6, pp. 527-539.

Arthur, J. R. [1951], Trans. Faraday Soc., 47, p. 164.

Avedesian, M. M. and J. F. Davidson [1973], Trans. Inst. Chem. Engrs., 51, pp. 121-131.

Batchelder, H. R., R. M. Busche and W. P. Armstrong [1953], Ind. and Eng. Chem., 45, 9, pp. 1856-1878.

Blake, T. R. [1976], Energy Research and Development Administration Report FE-1770-19.

Blake, T. R., S. K. Garg, H. B. Levine and J. W. Pritchett [1976], Energy Research and Development Administration Report FE-1770-15.

Dobner, S. [1976], Electric Power Research Institute Internal Report.

Essenhigh, R. H., R. Froberg and J. B. Howard [1965], Ind. Eng. Chem., 57, 9, pp. 33-43.

Field, M. A. [1969], Comb. and Flame, 13, pp. 237-257.

Field, M. A. [1970], Comb. and Flame, 14, pp. 237-248.

Field, M. A., D. W. Gill, B. B. Morgan, P. G. W. Hawksley [1967], Combustion of Pulverized Coal, BCURA, Leatherhead.

Golovina, E. S. and G. P. Khaustovich [1962], Eighth Int. Symp. Comb., pp. 784-792.

Gray, D., J. G. Cogoli and R. H. Essenhigh [1974], Adv. in Chemistry, 131, ACS, pp. 72-91.

Gray, M. D. and G. M. Kimber [1967], Nature, 214, pp. 797-798.

Hamor, R. J., I. W. Smith and R. J. Tyler [1973], Comb. and Flame, 21, pp. 153-162.

Harlow, F. H. and A. A. Amsden [1974], J. Comp. Phys., 61, pp. 1.

Hottel, H. C., G. C. Williams, N. M. Nerheim and G. R. Schneider [1965], Tenth Inter. Symp. Comb., pp. 111-121.

Keller, J. B. [1964], Proc. Symp. Appl. Math., XVI, Am. Math. Soc., pp. 145-170.

Kent, J. H. and R. W. Bilger [1973], Fourteenth Symp on Comb., pp. 615-625.

Kurylko, L. and R. H. Essenhigh [1972], Fourteenth Symp. on Comb., pp. 1375-1386.

Lane, F. [1967], General Applied Science Laboratories, Technical Report 645.

Launder, B. E. and D. B. Spalding [1972], Lectures in Mathematical Models of Turbulence, Academic Press, New York.

Libby, P. A. and F. A. Williams [1976], Annual Review of Fluid Mechanics, 8, pp. 351-376, Annual Reviews, Palo Alto.

Lewis, B. and G. von Elbe [1951], Combustion, Flames and Explosions of Gases, Academic Press, New York.

Marble, F. [1970], Annual Review of Fluid Mechanics, 2, pp. 397-446, Annual Reviews, Palo Alto.

Mulcahy, M. F. R. and I. W. Smith [1969], Rev. Pure and Appl. Chem., 19, pp. 81-108.

Nettleton, M. A. [1967], Ind. and Eng. Chem. Fund., 6, 1, pp. 20-25.

Penner, S. S. [1957], Chemistry Problems in Jet Propulsion, Pergammon, New York.

Peskin, R. L. [1974], Advances in Geophysics, 18, Academic Press, New York, pp. 141-163.

Rosner, D. E. [1972], Ann. Rev. Materials Sci., 2, pp. 573-606.

Schlichting, H. [1960], Boundary Layer Theory, McGraw-Hill, pp. 73-74.

Shapiro, A. H. and A. J. Erickson [1957], Trans. Am. Soc. Mech. Engr., 79, pp. 775-788.

Smith, I. W. [1971a], Comb. and Flame, pp. 303-314.

Smith, I. W. [1971b], Comb. and Flame, 17, pp. 421-428.

Thring, M. W. and R. H. Essenhigh [1963], Chemistry of Coal Utilization, Wiley, New York.

Tu, C. M., H. Davis and H. C. Hottel [1934], Ind. and Eng. Chem., 26, 9, pp. 749-757.

Walker, P. L., F. Rusinko and L. G. Austin [1959], Adv. Catalysis, 11, pp. 133-221.

Weisz, P. B. and C. D. Prater [1954], Adv. Catalysis, 6, pp. 143-196.

Wheeler, A. [1951], Adv. Catalysis, 3, pp. 249-327.

Williams, F. A. [1962], Eighth Symposium on Combustion, pp. 50-69.

Zienkiewicz, O. C. [1971], The Finite Element Method in Engineering Science, London.

☆U.S. GOVERNMENT PRINTING OFFICE: 1977-740-094